

MARCKS-like protein is an initiating molecule in axolotl appendage regeneration

Takuji Sugiura^{1,2†}, Heng Wang³, Rico Barsacchi², Andras Simon³ & Elly M. Tanaka^{1,2†}

Identifying key molecules that launch regeneration has been a long-sought goal. Multiple regenerative animals show an initial wound-associated proliferative response that transits into sustained proliferation if a considerable portion of the body part has been removed^{1–3}. In the axolotl, appendage amputation initiates a round of wound-associated cell cycle induction followed by continued proliferation that is dependent on nerve-derived signals^{4,5}. A wound-associated molecule that triggers the initial proliferative response to launch regeneration has remained obscure. Here, using an expression cloning strategy followed by *in vivo* gain- and loss-of-function assays, we identified axolotl MARCKS-like protein (MLP) as an extracellularly released factor that induces the initial cell cycle response during axolotl appendage regeneration. The identification of a regeneration-initiating molecule opens the possibility of understanding how to elicit regeneration in other animals.

To identify a regeneration-initiating molecule in the salamander *Ambystoma mexicanum* (axolotl), we aimed to functionally screen^{6,7} axolotl complementary DNAs using an *in vitro* salamander myotube cell cycle re-entry assay (*Notophthalmus viridescens*; newt)⁸ with the aim of performing *in vivo* analysis in the axolotl that is convenient for molecular analysis^{9–11}. To establish if axolotl blastema tissue expresses a myotube cell-cycle-entry inducing factor, we injected *Xenopus* oocytes with messenger RNAs from tail blastema, limb blastema or mature limb and assayed the extracellular media on myotubes (Fig. 1a). Tail or limb blastema mRNAs scored positively, comparable to serum, whereas the mature tissue mRNAs showed little inducing activity. We next screened an arrayed 6-day tail blastema cDNA eukaryotic expression vector library for the activity¹². Transfection of DNA representing the entire library as a single pool into HEK293 cells (Fig. 1b, sample WL) yielded cell media that stimulated myotube cell cycle entry (Fig. 1b). This library was fractionated into 12 superpools, which yielded four positive superpools (superpool numbers 6, 9, 10 and 12; Fig. 1b and Extended Data Fig. 1a–f). Sib-selection of superpool 9 through three subfractionation steps resulted in identification of a single clone responsible for the activity (Extended Data Fig. 2a–c).

The positive clone encoded a 224-amino-acid protein containing three conserved domains (myristoylated N terminus, MARCKS homology domain and effector domain) similar to MLP (Extended Data Fig. 3a) showing 74.1%, 68.0% and 80.0% amino acid sequence identity to human MLP (also known as MARCKSL1), including the glycine G2 in the myristoylated domain and two serines in the effector domain (S94 and S105) important for plasma membrane binding (for review see ref. 13). The C-terminal region showed low (14.4%) sequence conservation. Phylogenetic analysis showed that the axolotl sequence clustered with other vertebrate MLPs (Extended Data Fig. 3b).

Previous work in other species has indicated that MLP is an intracellular substrate for protein kinase C (PKC) associated with the plasma

membrane, phagocytic vesicles and actin, while phosphorylation by PKC induced dissociation to the cytoplasm (for review see ref. 14). We asked whether axolotl MLP (AxMLP) acted on myotubes as a secreted factor or whether it induced expression of a secreted factor in the HEK293 cells. To determine if AxMLP was extracellularly released, we transfected an expression plasmid encoding an AxMLP-C-terminal fusion with enhanced GFP (eGFP) or the pEGFP-N1 control construct into HEK293 cells (Extended Data Fig. 3c). Increasing levels of GFP fluorescence intensity were observed in *AxMlp-eGfp*-transfected but not *eGfp-N1*-transfected culture media (Fig. 1c). The percentage of GFP⁺ cells and the total cell number in *AxMlp-eGfp*- and *eGfp-N1*-transfected samples remained equivalent over time (Extended Data Fig. 3d, e). Time-lapse imaging further showed that *AxMlp-eGfp*-transfected cells grew similarly to the control cells (Supplementary Videos 1 and 2), indicating that extracellular AxMLP did not derive from dying cells. When comparing expression of AxMLP to zebrafish, *Xenopus*, mouse, newt and human MLPs in HEK293 cells, we observed that the AxMLP yielded a higher proportion of extracellular protein compared with other species (Fig. 1d). Bioassay of the axolotl versus newt MLP media induced a myotube response corresponding to the amount of protein seen by western blot (Fig. 1e).

To establish necessity, we exposed AxMLP-containing culture media to a polyclonal antibody against AxMLP that inhibited the myotube response, indicating that extracellular AxMLP is required for the activity (Fig. 1f and Extended Data Fig. 3f). To test sufficiency, we purified AxMLP-His, which displayed a characteristic high gel mobility (Extended Data Fig. 3g, h; for review see ref. 13). Exposure of myotubes to purified AxMLP in serum-free conditions yielded a robust myotube response with an approximate half-maximal response at 50.5 ng μ l⁻¹ (Fig. 1g and Extended Data Fig. 2d–f). We conclude that extracellular AxMLP is sufficient to induce myotube cell cycle re-entry.

To determine the *in vivo* function of extracellular AxMLP, we first queried whether purified AxMLP protein injected into uninjured axolotl tail (Fig. 2) and limb (Extended Data Fig. 4) tissue was sufficient to induce cell cycle re-entry. We injected 270 ng of AxMLP followed by injection of 5-bromodeoxyuridine (BrdU) at 3 days post-amputation (dpa) (Fig. 2a and Extended Data Fig. 4e). AxMLP-injected tails contained significantly more BrdU-positive cells (18.9 ± 2.59%) than control tails injected with media depleted of AxMLP (flow-through, 3.20 ± 0.863%; PBS, 3.04 ± 1.00%) (Fig. 2b–d). AxMLP injection caused increased BrdU uptake in all counted cell types in limbs and tails except for myocyte enhancer factor 2C (MEF2C)⁺ muscle nuclei (Fig. 2b–d and Extended Data Fig. 4a–d, f–n). Interestingly, it was recently found that muscle fibres can dedifferentiate during newt limb regeneration, but not in axolotl¹⁵. The responsiveness of axolotl PAX7⁺ satellite cells but not MEF2C⁺ muscle nuclei to AxMLP corresponds with PAX7⁺ satellite cells being the main contributors to muscle regeneration in axolotl¹⁵.

¹DFG Research Center for Regenerative Therapies (CRTD), Technische Universität Dresden, Fetscherstrasse 105, 01307 Dresden, Germany. ²Max Planck Institute for Molecular Cell Biology and Genetics, Pfotenhauerstrasse 108, 01307 Dresden, Germany. ³Karolinska Institute, Department of Cell and Molecular Biology, Centre of Developmental Biology for Regenerative Medicine, SE-171 77 Stockholm, Sweden. [†]Present address: DFG Research Center for Regenerative Therapies, Technische Universität Dresden, Fetscherstrasse 105, 01307 Dresden, Germany.

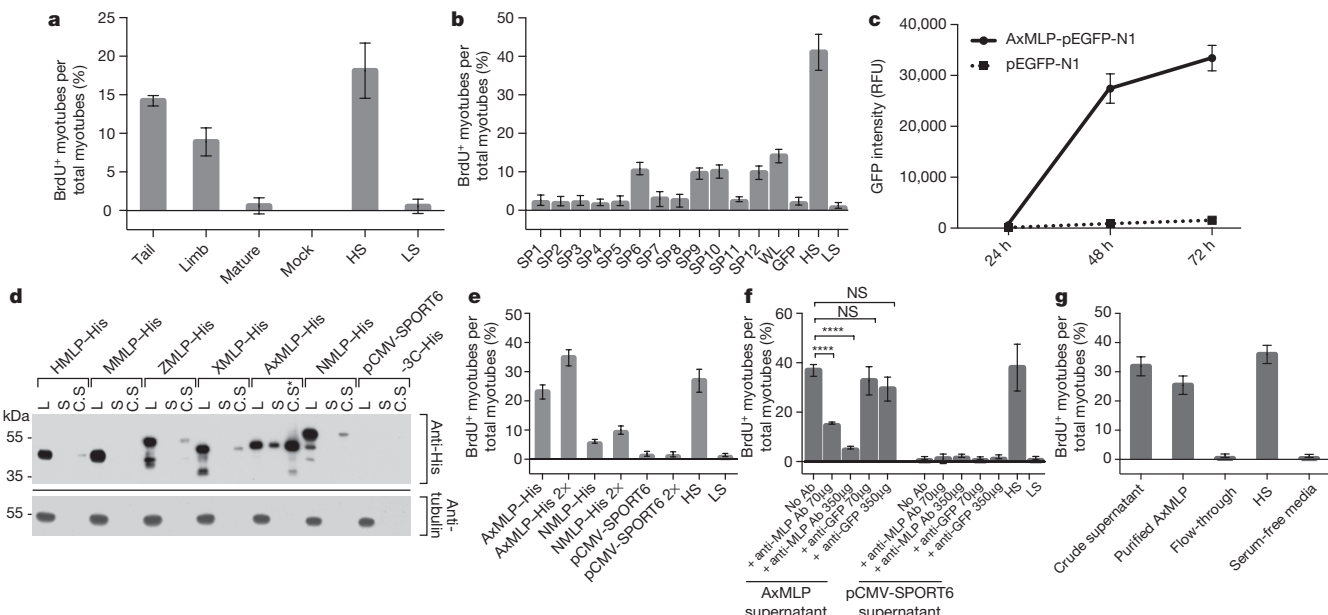


Figure 1 | Extracellular AxMLP identified by expression cloning is necessary and sufficient for cell cycle re-entry *in vitro*.

a, Supernatants from *Xenopus* oocytes injected with total mRNA from tail and limb blastema induced robust BrdU incorporation in cultured newt myotubes (myotube assay) ($n = 6$: 2 biological, 3 technical replicates each; mean \pm standard deviation (s.d.)). b, A screen for the cell-cycle-inducing clone. Culture media from HEK293 cells transfected with 6-day tail blastema cDNA library pools and assayed on myotubes for cell cycle induction (see Extended Data Fig. 1 for scheme) identified four positive superpools ($n = 12$: 4 biological, 3 technical replicates each; mean \pm s.d.). Superpool 9 was sub-selected to a single clone (see Extended Data Fig. 2a–c). c, AxMLP-GFP fusion protein detection in culture media of transfected HEK293 cells by fluorescence luminometry ($n = 3$: biological replicates; mean \pm s.d.). RFU, relative fluorescence units. d, MLP orthologues show

As we had used the newt myogenic cell line for the original screen, we asked whether AxMLP could promote *in vivo* cell cycle entry during muscle dedifferentiation in the newt. AxMLP protein

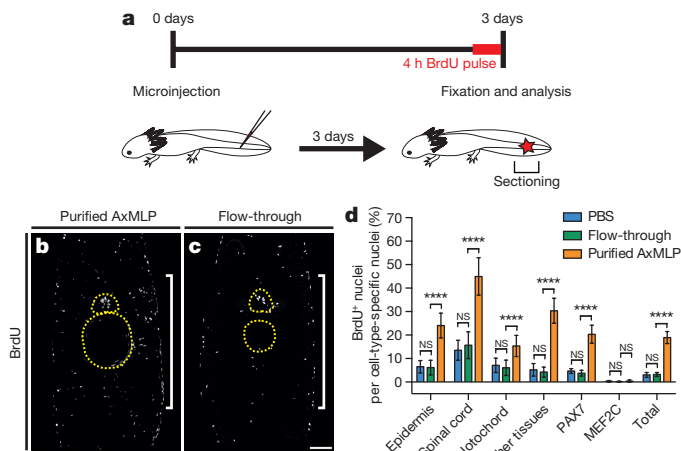


Figure 2 | AxMLP is sufficient to induce cell cycle entry *in vivo*.

a, Schematic illustration of *in vivo* protein injection experiment. b, c, Transverse sections of tails injected with purified AxMLP (b) or flow-through (fraction depleted of AxMLP) (c) immunostained for BrdU. Yellow circles indicate spinal cord (top) and notochord (bottom); white brackets indicate injection site. Scale bar, 200 μ m. d, Quantification of BrdU⁺ cells in injected tails. Quantification of BrdU⁺/PAX7⁺ cells and BrdU⁺/MEF2C⁺ cells shows that AxMLP induces cell cycle entry in PAX7⁺ cells. NS, not significant; ***P < 0.0001 with Student's *t*-test ($n = 15$: 5 biological, 3 technical replicates each; mean \pm s.d.).

differing levels of extracellular protein. AxMLP was readily detectable by western blotting in cell culture supernatant (S). Human (HMLP), zebrafish (ZMLP), *Xenopus* (XMLP) and newt (NMLP) MLP were only detectable in 40-fold concentrated supernatants (C.S.). Asterisk indicates fivefold concentrated supernatant. Loading control: anti-tubulin. e, AxMLP and NMLP supernatants both induce myotube cell cycle with response corresponding to protein levels in supernatant ($n = 6$: 2 biological, 3 technical replicates each; mean \pm s.d.). f, Induction of myotube cell cycle re-entry by AxMLP is specifically blocked by addition of polyclonal anti-AxMLP antibodies (Ab) to culture supernatant ($n = 6$: 2 biological, 3 technical replicates each; mean \pm s.d.). g, Purified AxMLP induces myotube cell cycle re-entry ($n = 6$: 2 biological, 3 technical replicates each; mean \pm s.d.). HS, high serum; L, cell lysate; LS, low serum; SP, superpool; WL, whole library. ***P < 0.0001 with Student's *t*-test. NS, not significant.

was injected either into uninjured newt limbs or after limb amputation during the muscle dedifferentiation phase (Fig. 3). Injection of AxMLP into uninjured newt tissue was not sufficient to induce a cell cycle response (Fig. 3a). Injection during regeneration, however, resulted in an increased 5-ethynyldeoxyuridine (EdU) uptake in PAX7⁺ satellite cells as well as dedifferentiating myofibre-derived cells (Fig. 3b, c)¹⁵. These data indicate that AxMLP can also promote cell cycle entry of at least two cell types in newt, including dedifferentiating muscle. The requirement for an additional injury signal to induce cell cycle entry in newt correlates with a higher propensity of axolotl stem cells to cycle in homeostasis compared with their newt counterparts^{16,17}.

We next asked if AxMLP is important for cell proliferation during axolotl regeneration. Microarray and quantitative reverse transcription polymerase chain reaction (qRT-PCR) detected expression in mature limb and tail tissue followed by upregulation with a peak of expression at 12 to 24 h post-amputation (hpa), returning to basal levels at 2 dpa in the tail and 4 dpa in the limb (Extended Data Fig. 5a, e). These observations are consistent with a role for AxMLP in early events of regeneration. Protein localization using immunofluorescence showed that in uninjured tissue, AxMLP was cytoplasmically localized in epidermis and in tail spinal cord cells, including radial glia and axonal tracts (Extended Data Fig. 5b, f, high-magnification images). At 1 and 6 dpa, expression was maintained in the epidermis and spinal cord (Extended Data Fig. 5c, d, g, h, high-magnification images). However, the protein in the regenerating wound epidermis at 1 dpa was plasma-membrane associated (Extended Data Fig. 5c, g, green arrowheads in high magnification images). Such localization changes have previously been described for MARCKS proteins and are dependent on phosphorylation state¹⁸. In summary, AxMLP protein is

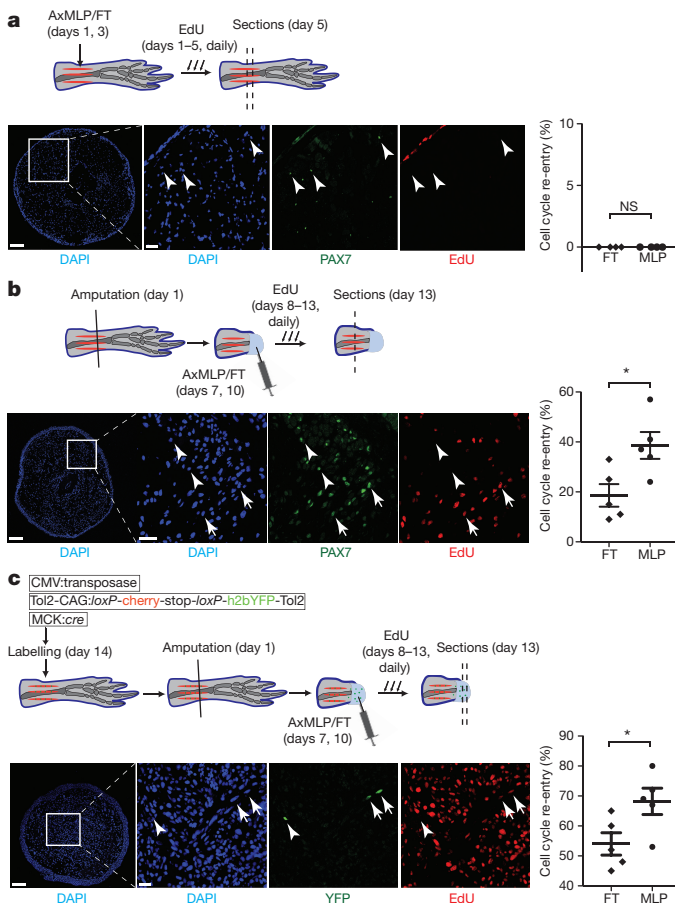


Figure 3 | AxMLP induces cell cycle re-entry of muscle-derived cells in the newt limb. **a–c,** Top, schematic representation of the experimental paradigm testing the effect of AxMLP on PAX7⁺ satellite cell proliferation in uninjured limb (**a**), on PAX7⁺ satellite cell activation in injured limb (**b**) or myofibre dedifferentiation after injury (**c**). **a,** Bottom, transverse section of uninjured limb injected with purified AxMLP shows no induction of EdU incorporation. Graph showing no difference in either purified AxMLP- or flow-through- (FT) injected uninjured limbs (right; $n = 4$; biological replicates). **b,** Bottom, transverse section of the regenerating limb injected with AxMLP shows increased EdU incorporation of PAX7⁺ cells. Graph showing more EdU⁺/PAX7⁺ satellite cells in AxMLP-injected limbs (right; $n = 5$; biological replicates; mean \pm standard error of the mean (s.e.m.)). **c,** Bottom, transverse section from myofibre-labelled, regenerating limb injected with AxMLP. Graph showing more EdU⁺/yellow fluorescent protein (YFP)⁺ myofibre progeny in AxMLP-injected blastemas (right; $n = 5$; biological replicates; mean \pm s.e.m.). NS, not significant; * $P < 0.05$ with Student's *t*-test. Scale bars in lower-magnification images, 200 μm ; in higher-magnification images, 20 μm . Arrowheads indicate marker⁺/EdU[−] cells; arrows indicate marker⁺/EdU⁺ cells. DAPI, 4',6-diamidino-2-phenylindole.

cytoplasmically localized in mature tissue. Upon amputation, mRNA levels rise by at least eightfold. Concomitantly the AxMLP protein in the wound epidermis shows juxtamembrane localization, consistent with its N-terminal myristylation sequence and suggestive of extracellular release. These data suggest that both the level and intracellular localization are critical in the role of AxMLP as a non-autonomous inducer of initial cell cycles. A detailed understanding of the different cytoplasmic pools and their relationship to the extracellular form will require further study.

To test the function of endogenous AxMLP during regeneration, we implemented two different fluorescein isothiocyanate (FITC)-conjugated morpholinos directed against 5' sequences of the *AxMlp* mRNA. We validated the effectiveness of the morpholinos *in vitro* by co-electroporation with plasmid encoding full-length *AxMlp* or

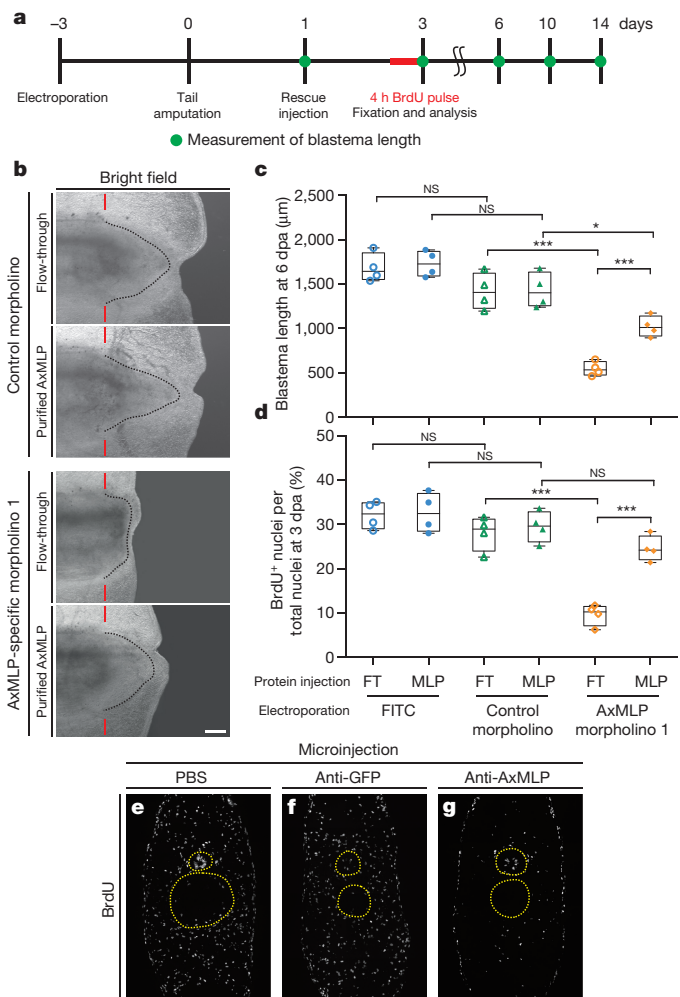


Figure 4 | AxMLP is necessary for cell proliferation during early tail regeneration. **a,** Schematic diagram of the morpholino electroporation experiment. **b,** Bright-field images of the morpholino-electroporated/protein-injected tails at 6 dpa showing inhibition of regeneration by anti-*AxMlp* morpholino and rescue by protein injection. Scale bar, 500 μm . Red bars indicate amputation planes; dashed lines delineate shape of the blastema. **c,** Blastema length at 6 dpa. The sample order on the x-axis is the same as in **d** ($n = 4$; biological replicates; centre values as median; points represent each sample). FT, flow-through. **d,** Quantification of BrdU⁺ cells in tail blastema sections at 3 dpa ($n = 4$; biological replicates; centre values as median; points represent each sample). **e–g,** Injection of anti-AxMLP antibody inhibits proliferation after tail amputation. Transverse sections of 3-day regenerating tails that had been injected with PBS (**e**), anti-GFP antibody (**f**) or anti-AxMLP antibody (**g**) (for details see Extended Data Fig. 9). Sections immunostained for BrdU. * $P < 0.05$, *** $P < 0.0005$ with Student's *t*-test. Scale bar, 200 μm . Yellow circles delineate the spinal cord (top) and notochord/cartilage (bottom).

Δ N-terminal-*AxMlp*-His lacking the target sequence into cultured newt cells (Extended Data Fig. 6a, k). Immunostainings and western blots showed that the morpholinos strongly reduced AxMLP expression but did not affect the expression of Δ N-AxMLP (Extended Data Fig. 6b–j, l–s). No effects were observed with two different negative control morpholinos including a five-mismatch morpholino (Extended Data Fig. 6b–j, l–s).

To knockdown AxMLP *in vivo*, we electroporated *AxMlp* or control morpholinos into the tail epidermis and spinal cord 3 days before amputation. Reduction of protein levels in electroporated cells was confirmed by immunostaining (Extended Data Fig. 7). To test whether exogenously provided AxMLP protein would rescue the knockdown phenotype, the electroporated tails were injected at 1 dpa with purified

AxMLP or inactive flow-through. Blastema length was measured at 1, 3, 6, 10 and 14 dpa, and BrdU incorporation was assayed at 3 dpa (Fig. 4a and Extended Data Fig. 8f, i). Incorporation of BrdU in the *AxMlp* morpholino-electroporated samples was significantly reduced (Fig. 4d and Extended Data Fig. 8a–e). Correspondingly, at 6 dpa, the blastema length of the *AxMlp*-morpholino/flow-through-injected tails was 59% smaller than that of the control morpholino/flow-through-injected ones (specific/flow-through, $546.7 \pm 80.1 \mu\text{m}$; control/flow-through, $1,318 \pm 206 \mu\text{m}$; Fig. 4b, c). In contrast, *AxMlp*-morpholino-electroporated tails injected with purified AxMLP protein showed a 50% rescue in blastema length and 85% rescue of BrdU incorporation (Fig. 4c, d). The partial rescue in blastema length is probably due to the limited amounts of AxMLP provided by a single injection. The specificity of the phenotype was confirmed by implementing the second morpholino and the control five-mismatch morpholino (Extended Data Fig. 8g–j). These results show that knockdown of AxMLP via morpholino results in reduced cell proliferation that can be rescued by provision into the muscle/blastema tissue of exogenous AxMLP protein.

To corroborate the morpholino experiments, we injected the anti-AxMLP blocking antibody into the tail before and during regeneration (Extended Data Fig. 9a), which strongly reduced BrdU incorporation in multiple tissues (Fig. 4e–g and Extended Data Fig. 9b). These results show that *in vivo* knockdown of AxMLP activity by two methods resulted in reduced cell proliferation during early regeneration. To determine if an excess of AxMLP could accelerate regeneration, we performed multiple injections of AxMLP protein before and during early phases of regeneration (Extended Data Fig. 10a). The oversupply of protein resulted in a larger blastema at 4 dpa (Extended Data Fig. 10b, c).

This work represents the first identification of a molecule, AxMLP, by functional expression cloning and *in vivo* testing in appendage regeneration and therefore sets an experimental paradigm for future studies. Previous work indicated that spinal cord neural stem cells accelerate their cell cycle kinetics resulting in increased mitoses between 3 and 4 dpa (ref. 19). Our work indicates that AxMLP is a major factor responsible for the induction of these cell cycle kinetics. How AxMLP is delivered extracellularly, its mode of intracellular signalling and whether orthologues beyond salamanders are associated with regenerative events will be important topics of future investigation.

Online Content Methods, along with any additional Extended Data display items and Source Data, are available in the online version of the paper; references unique to these sections appear only in the online paper.

Received 21 December 2014; accepted 7 January 2016.

Published online 2 March 2016.

- Wenemoser, D. & Reddien, P. W. Planarian regeneration involves distinct stem cell responses to wounds and tissue absence. *Dev. Biol.* **344**, 979–991 (2010).
- Knapp, D. et al. Comparative transcriptional profiling of the axolotl limb identifies a tripartite regeneration-specific gene program. *PLoS ONE* **8**, e61352 (2013).
- Tassava, R. A. & Mescher, A. L. The roles of injury, nerves, and the wound epidermis during the initiation of amphibian limb regeneration. *Differentiation* **4**, 23–24 (1975).
- Endo, T., Bryant, S. V. & Gardiner, D. M. A stepwise model system for limb regeneration. *Dev. Biol.* **270**, 135–145 (2004).

- Holtzer, S. The inductive activity of the spinal cord in urodele tail regeneration. *J. Morphol.* **99**, 1–39 (1956).
- Julius, D., MacDermott, A. B., Axel, R. & Jessell, T. M. Molecular characterization of a functional cDNA encoding the serotonin 1c receptor. *Science* **241**, 558–564 (1988).
- Yang, Y. C. et al. Human IL-3 (multi-CSF): identification by expression cloning of a novel hematopoietic growth factor related to murine IL-3. *Cell* **47**, 3–10 (1986).
- Tanaka, E. M., Gann, A. A., Gates, P. B. & Brockes, J. P. Newt myotubes reenter the cell cycle by phosphorylation of the retinoblastoma protein. *J. Cell Biol.* **136**, 155–165 (1999).
- Khattak, S. et al. Foamy virus for efficient gene transfer in regeneration studies. *BMC Dev. Biol.* **13**, 17 (2013).
- Khattak, S. et al. Germline transgenic methods for tracking cells and testing gene function during regeneration in the axolotl. *Stem Cell Reports* **1**, 90–103 (2013).
- Schnapp, E. & Tanaka, E. M. Quantitative evaluation of morpholino-mediated protein knockdown of GFP, MSX1, and PAX7 during tail regeneration in *Ambystoma mexicanum*. *Dev. Dyn.* **232**, 162–170 (2005).
- Gruber, C. E. Production of cDNA libraries by electroporation. *Methods Mol. Biol.* **47**, 67–79 (1995).
- Sundaram, M., Cook, H. W. & Byers, D. M. The MARCKS family of phospholipid binding proteins: regulation of phospholipase D and other cellular components. *Biochem. Cell Biol.* **82**, 191–200 (2004).
- Aderem, A. The MARCKS brothers: a family of protein kinase C substrates. *Cell* **71**, 713–716 (1992).
- Sandoval-Guzmán, T. et al. Fundamental differences in dedifferentiation and stem cell recruitment during skeletal muscle regeneration in two salamander species. *Cell Stem Cell* **14**, 174–187 (2014).
- Berg, D. A. et al. Efficient regeneration by activation of neurogenesis in homeostatically quiescent regions of the adult vertebrate brain. *Development* **137**, 4127–4134 (2010).
- Maden, M., Manwell, L. A. & Ormerod, B. K. Proliferation zones in the axolotl brain and regeneration of the telencephalon. *Neural Dev.* **8**, 1 (2013).
- Seykora, J. T., Myat, M. M., Allen, L. A., Ravetch, J. V. & Aderem, A. Molecular determinants of the myristoyl-electrostatic switch of MARCKS. *J. Biol. Chem.* **271**, 18797–18802 (1996).
- Rodrigo Albors, A. et al. Planar cell polarity-mediated induction of neural stem cell expansion during axolotl spinal cord regeneration. *eLife* **4**, e10230 (2015).

Supplementary Information is available in the online version of the paper.

Acknowledgements We thank A. Tazaki, Y. Taniguchi, I. Wagner, A. Rodrigo-Albors, D. Knapp, P. Murawala, B. Borgonovo and D. Drechsel for technical advice and important discussions; M. Schuez, A. Telzerow and Y. Taniguchi for assistance; B. Gruhl, A. Wagner, S. Mögel for animal care; and J. Currie, T. Sandoval-Guzman and E. Nacu for comments on the manuscript. E.M.T. was supported by a German Federal Ministry of Education and Research (BMBF) Biofutures grant, German Research Foundation (DFG) grant TA274/5-1, European Research Council Advanced Grant, Institutional funding from the Max Planck Institute of Molecular Cell Biology and Genetics (MPI-CBG), and the DFG Research Center for Regenerative Therapies Dresden (CRTD) and A.S. by the Swedish Research Council and Cancerfonden.

Author Contributions R.B. performed oocyte injection assay and established expression cloning. T.S. designed and performed expression cloning, *in vitro* cell assays, biochemical experiments, *in vivo* axolotl experiments, analysed experiments and data, and wrote the manuscript. E.M.T. conceived of the project, analysed experiments and data, wrote the manuscript and secured funding. H.W. designed and performed *in vivo* newt experiments, analysed the data and wrote the corresponding parts of the manuscript. A.S. supervised and designed *in vivo* newt experiments, analysed data, edited the manuscript and secured funding.

Author Information The sequence of AxMLP has been deposited in the NCBI GenBank database under accession number KT367888. Reprints and permissions information is available at www.nature.com/reprints. The authors declare no competing financial interests. Readers are welcome to comment on the online version of the paper. Correspondence and requests for materials should be addressed to E.M.T. (elly.tanaka@crt-dresden.de) or T.S. (takuji.sugiura@crt-dresden.de).

METHODS

Animals. All animal experiments were performed in accordance with the European Community and local ethics committee guidelines. *Xenopus laevis* were purchased (Nasco) and maintained in our animal facility. *Ambystoma mexicanum* (axolotls) were bred and maintained in our facility, where they were kept at 18 °C in Dresden tap water and fed daily with artemia or fish pellets. Five-to-six centimetre (snout to tail tip) axolotls were used for all the experiments. Animals were anaesthetized for all the surgical process as previously described²⁰. Labelling of connective tissue was achieved by transplanting lateral plate mesoderm from GFP transgenic embryos to normal host embryos as previously described²⁰.

Protein expression by *Xenopus* oocytes. Total RNA was isolated from day-1, day-3 and day-5 limb and tail blastemas with TRIzol reagent (Invitrogen) according to the manufacturer's manual. Total RNA from mature (not regenerating) limb tissues was isolated using the same procedure as blastema samples. Blastema RNAs from the different time points were equivalently pooled as limb-blastema total RNA or tail-blastema total RNA, respectively. mRNA was purified from limb-blastema or tail-blastema total RNA with the Poly (A) Quick mRNA isolation kit (Stratagene). *Xenopus* oocyte preparation and microinjection were performed essentially as previously described^{6,7,21}. Briefly, mature oocytes were defolliculated with collagenase (Sigma). Purified mRNA (5.0 ng) was injected into the selected healthy oocytes after the defolliculation. Eight injected oocytes were cultured together in one well of a 96-well plate (Nunc) for 48 h and the supernatants were harvested for myotube assay (see later).

Functional expression cloning. Clones (110,592) from a 6-day tail blastema library were arrayed into 288 × 384-well plates²². To prepare the 'pools', all the saturated bacterial cultures on one 384-well plate were pooled in one conical tube, and 288 pools were prepared from the library in total. To prepare the 'superpools', 24 pools were combined together in one conical tube, and 12 superpools were prepared from the pools in total (Extended Data Fig. 1a–c). To obtain superpool plasmid, 500 µl of superpool bacteria were cultured in 50 ml LB medium (Extended Data Fig. 1d). To avoid losing low frequency clones in the superpools, the optical density (OD) of each culture was controlled and the cultures were harvested around OD_{600 nm} 0.6. Superpool plasmids were purified with QIAGEN Plasmid Midi Kit (QIAGEN) according to the manufacturer's manual. To reconstitute the whole library, 5 µg of each superpool's plasmids were pooled in one tube before transfection. HEK293FT cells (Invitrogen) were maintained with the standard protocol from Invitrogen. To obtain the superpool supernatants, 8.0 × 10⁵ of HEK293 cells were plated on one well of a 6-well plate (Nunc) and 1 µg of each individual superpool plasmids were transfected into HEK293 cells with Fugene 6 (Roche; Extended Data Fig. 1e) according to the manufacturer's manual. For the first 24 h, the transfected HEK293 cells were kept in the 10% fetal calf serum (FCS) medium. Then the cells were rinsed with FreeStyle 293 expression medium (Gibco) that is a serum-free medium and cultured in the medium at 72 h after transfection. Individually harvested supernatants were concentrated approximately tenfold with a Vivaspin 10,000 MWCO (Sartorius). These concentrated supernatants were tested on A1 myotubes (Extended Data Fig. 1f). It should be noted that given the injury-specific extracellular activity of AxMLP, we infer that the *Xenopus* oocyte and HEK293 cell systems are likely to be in 'wound-epithelium-like' signalling states that permit at least some extracellular release of AxMLP, and that the 6-day regenerating tail blastema cDNA had a sufficient number of AxMLP clones for detection in the expression cloning system. We only detected 1 AxMLP clone among 100,000 clones, and this may reflect the levels of mRNA present at later regeneration time points.

Maintenance of A1 myoblasts, myotube differentiation from A1 myoblasts, myotube purification and subsequent myotube assays were performed essentially as described previously^{8,23,24}. Briefly, concentrated supernatants were individually added into myotube culture medium in a 96-well plate and incubated for 5 days, and BrdU (Sigma; final 10 µg ml⁻¹) was added to the culture media for 18 h before the fixation with 1.5% PFA (Sigma)/PBS. Fixed myotubes were stained with anti-MHC and anti-BrdU antibodies (mouse monoclonal, 4a1025 and Bu20a) conjugated to FITC or rhodamine with DyLight Antibody Labelling Kit (Thermo Scientific) according to the manufacturer's manual. For the quantification of BrdU incorporation activity, the total number of myotubes and BrdU⁺ myotubes were counted by hand under the microscope (Zeiss Axioplan 2). This biological evaluation of the BrdU-incorporation activity on myotubes is called the myotube assay. The high-serum (15% FCS) condition was used as a positive control for myotube assays and the low-serum (0.5% FCS) or serum-free condition was used as a negative control.

For the second screen from superpool number 9, the clones from the 24 384-well plates contained in superpool 9 were divided into smaller sub-pools according to a two-dimensional matrix (Extended Data Fig. 2a). For example, sub-pool A contained pools from plates 193–198 and sub-pool 1 contained pools from plates 193, 199, 205, 211. These sub-pools were cultured to OD_{600 nm} 0.6 before plasmid

preparation. For the third screen from pool number 212, 384 single clones were arrayed by 96-pin plastic replicators (Genetix) on 96-well plates (SARSTEDT) filling 150 µl LB medium per well (Extended Data Fig. 2b; groups A–D). Individual clones on the 96-well plates were statically cultured until they were saturated and 24 clones were pooled together (Extended Data Fig. 2b; sub-pools A1–D4). Plasmids from each pool were purified with QIAprep spin miniprep kit (QIAGEN). For the fourth screen from A1, 24 clones were individually cultured in LB medium and the plasmids were purified with QIAprep spin miniprep kit (QIAGEN). To construct sub-pools, 1 µg of the plasmid from each single clone was pooled according to the diagram in Extended Data Fig. 2c. The process from the transfection into HEK293 cells to myotube assay in the second to the fourth screen was the same as the first screen. To validate transfection efficiency during whole expression cloning, 50 pg of secreted alkaline phosphatase (SEAP)-pCMV-SPORT6 plasmid was co-transfected with the samples as a spike and a portion of the supernatants was assayed by Great EscAPE SEAP Chemiluminescence Kit 2.0 (Clontech). The luminescence of the supernatants was measured by GENiosPro Microplate Reader (TECAN). We confirmed that there was no significant difference of transfection efficiency during the expression cloning (data not shown). There were no cell line misidentification and cross-contamination in the experiments. We used a single mammalian cell line (HEK293FT cells) provided by Invitrogen and single amphibian cell line (newt A1 cells) in the experiments. These two cell lines have totally different morphologies and are cultured under mutually incompatible culture conditions. The growth of both cells were carefully monitored during the experiments and cells samples were constantly stained with Hoechst 33342 (Sigma, final 0.5 µg ml⁻¹) to test mycoplasma contamination.

Plasmid construction. Human and mouse *MLP* cDNA clones were purchased from OriGene Technologies (clone ID: human, SC112373; mouse, MC208965). Zebrafish and *Xenopus* *mlp* cDNA clones were purchased from Source BioScience (clone ID: zebrafish, 6795591; *Xenopus*, 8330180). All oligonucleotide sequences and the restriction enzyme sites using for cloning are shown in Supplementary Table 2. Since the backbone vector of the cDNA library is pCMV-SPORT6, we subcloned following genes into pCMV-SPORT6 vector (Invitrogen) or pCMV-SPORT6-3C-His vector. PCR-amplified fragments with the oligonucleotides numbers 1 and 2 from pSEAP2-Basic (Clontech) were subcloned into pCMV-SPORT6. The oligonucleotides numbers 3 and 4 were attached to pCMV-SPORT6 to generate a backbone vector, pCMV-SPORT6-3C-His (Extended Data Fig. 3c, bottom left). The *AxMlp* open reading frame (ORF) was amplified by PCR with the oligonucleotides numbers 5 and 6 from the original *AxMlp* clone (*BL212a101*) and subcloned in the pCMV-SPORT6-3C-His vector (Extended Data Fig. 3c, top left). N-terminal deletion *AxMlp* was amplified by PCR with the oligonucleotides numbers 7 and 8 from the original *AxMlp* clone (*BL212a101*) and subcloned in the pCMV-SPORT6-3C-His vector (Extended Data Fig. 6a, bottom). Human, mouse, zebrafish and *Xenopus* *MLP* ORFs were amplified from purchased cDNA clones with specific primers (for human, oligonucleotides numbers 9, 10; mouse, oligonucleotides numbers 9, 11; zebrafish, oligonucleotides numbers 12, 13; *Xenopus*, oligonucleotides numbers 14, 15, respectively), and were subcloned in the pCMV-SPORT6-3C-His vector. The oligonucleotides numbers 16 and 17 were inserted into the pEGFP-N1 plasmid (Clontech) to generate a backbone vector, pEGFP-N1-3C (Extended Data Fig. 3c, bottom right). The *AxMlp* ORF was amplified by PCR with the oligonucleotides numbers 18 and 19 from the original *AxMlp* clone (*BL212a101*) and subcloned into pEGFP-N1-3C (Extended Data Fig. 3c, top right). Newt *Mlp* ORF was amplified by PCR from newt limb blastema cDNA with the oligonucleotides numbers 28 and 29 and the PCR fragments were subcloned in the pCMV-SPORT6-3C-His vector. These constructs were confirmed by sequencing.

Assessment of AxMLP extracellular secretion. For measuring the GFP intensity of supernatants, 8.0 × 10⁵ of HEK293 cells were plated on 6-well plates and 1 µg of *AxMLP*-3C-pEGFP-N1 plasmid or 1 µg of empty-pEGFP-N1 plasmid were transfected into HEK293 cells. The supernatants were harvested at 24 h post-transfection (hpt), 48 hpt and 72 hpt and concentrated with Vivaspin 10,000 MWCO (Sartorius) individually. The fluorescence intensity was measured using a GENiosPro Microplate Reader (TECAN). To determine the percentage of GFP⁺ cells in the culture, the transfected cells were detached with Trypsin-EDTA (Gibco, final 0.05%)/PBS from the well, then spread on improved Neubauer chamber. The number of GFP⁺ cells and total cells in the grids were counted by hand and the percentage was calculated. Time-lapse imaging was performed under Axiovert 200M (Zeiss) with humidity, temperature and CO₂ control chamber. Images were taken every 30 min from 5 to 72 hpt.

Antibody blocking. For the antibody-based blocking assay *in vitro*, 1 µg of *AxMlp*-3C-His-pCMV-SPORT6 plasmid or empty-pCMV-SPORT6-3C-His plasmid was transfected into HEK293 cells with Fugene 6 (Roche). The supernatants were harvested at 72 hpt and concentrated. Ten micrograms of AxMLP-3C-His protein

(22.7 kDa) were treated with 70 µg or 350 µg of anti-AxMLP polyclonal antibody (see later) or anti-GFP polyclonal antibody (MPI-CBG antibody facility) as a negative control, respectively, at room temperature for 2 h. These antibody-treated supernatants were used for the myotube assay.

For the *in vivo* antibody blocking assay, anti-full-length AxMLP polyclonal antibody (see later), anti-GFP polyclonal antibody (MPI-CBG antibody facility) or PBS as a negative control were injected into mature (not regenerating) tail as the first injection (3 h before amputation) and injected into the blastema as the second injection (12 h post-amputation) and as the third injection (1 day post-amputation) (Extended Data Fig. 9a). These samples were co-injected with tetramethylrhodamine dextran MW 70,000 (Molecular Probes; final 2.5 mg ml⁻¹) as a tracer. The injection efficiency was confirmed based on the intensity of the rhodamine under the fluorescence dissecting microscope (SZX 16, OLYMPUS). No animals were excluded from the analysis. In each injection 500 ng, then, in total 1.5 µg antibody or equivalent volume of PBS were injected. Injected animals were kept in clean tap water for 3 days at room temperature. The animals were injected intraperitoneally with 30 µl of 2.5 mg ml⁻¹ BrdU (Sigma) 4 h before collecting the tails. The injected blastemas were fixed, embedded, cryosectioned and immunostained as described later. For the imaging, the tiled images of the entire cross-section of the tails taken on a Zeiss Observer.Z1 (Zeiss) were then stitched by Axiovision software or Zen 2 (Zeiss). For the quantification at least a total of 1,000 cells per one animal were counted from four different animals in each condition (PBS, anti-GFP antibody or anti-AxMLP injection, respectively), and the marker-positive nuclei (BrdU⁺, PAX7⁺, MEF2⁺ or Hoechst⁺) on the sections were counted by hand. The cells in spinal cord, epidermis and cartilage/notochord were separately counted based on morphology. The label "Other tissues" in Fig. 2d, contained mainly mesenchymal cells and endothelial cells and was calculated by the subtraction from the total number to the number of all the other specific cell types.

AxMLP purification. For His-tagged AxMLP purification, AxMLP-3C-His-pCMV-SPORT6 plasmid was transfected into HEK293 cells and the supernatant was harvested at 72 hpt. His-tagged protein in the supernatant was purified in native conditions on a 1 ml HisTrap HP column (GE Healthcare) using FreeStyle 293 expression medium including 500 mM imidazole step elution. The eluate (purified AxMLP) and depleted media (flow-through) were concentrated with Vivaspin 10,000 MWCO (sartorius) 40 fold and the final concentration of purified AxMLP was 1.31 µg µl⁻¹. Both concentrated eluate (purified AxMLP) and flow-through fractions were dialysed with Spectra/Por Dialysis Membrane MWCO 6-8000 (Spectrum Laboratories) in AMEM (MEM medium (Gibco) diluted 25% with distilled water) for biological assays. The fractions from the purification were tested by silver staining and western blotting (Extended Data Fig. 3g, h). The washing fraction was concentrated about tenfold to load the same volume as other fractions on 4–20% gradient SDS-PAGE gels (anamed Elektrophoresis). Western blotting and silver staining were performed with a standard protocol. Briefly, the fractions were treated with 2× Sample Buffer including dithiothreitol (DTT; Sigma, final 0.2 M) and boiled at 95 °C for 10 min. The proteins were blotted onto PROTRAN nitrocellulose transfer membrane (Whatman) by TE 77 Semi-Dry Transfer Unit (Amersham). The membrane was blocked with 5% skim milk. Primary antibodies used: mouse anti-His (QIAGEN, 1/5,000), mouse anti-α-tubulin (MPI-CBG antibody facility, DM1A 1/5,000), rabbit anti-AxMLP-full length (1/2,500), rabbit anti-AxMLP-C terminus (1/2,500). Secondary antibodies used: goat anti mouse-HRP (Jackson ImmunoResearch Laboratories, 1/5,000), goat anti rabbit-HRP (Jackson ImmunoResearch Laboratories, 1/5,000). Cell lysates for western blotting were obtained by directly adding 2× Sample Buffer on top of the cultured cells and were boiled at 95 °C for 10 min.

Antibodies and immunohistochemistry. For the preparation of anti-full-length AxMLP polyclonal antibody, a glutathione S-transferase (GST) fusion protein with full-length amino acids of AxMLP was expressed in bacteria and purified by standard methods on GS-trap, glutathione sepharose (GE Healthcare). Purified GST fusion protein as an antigen was used to immunize rabbits (Charles River). Anti-serum was affinity purified using maltose-binding protein fused with full-length AxMLP conjugated to NHS-Sepharose resin (GE Healthcare). To raise C-terminal AxMLP polyclonal antibody, keyhole limpet haemocyanin (KLH)-tagged peptides, PPVEPQVEEVAAPAP, was used to immunize rabbits and the affinity-purified polyclonal antibody was provided (Eurogentec). Both anti-full-length and anti-C-terminal AxMLP polyclonal antibodies were tested on the cell lysate from AxMLP-transfected HEK293 cells (Extended Data Fig. 3f).

Limb blastema and tail blastema preparations for sectioning were produced essentially as previously described²⁵. Briefly, limb blastemas amputated at the wrist level were collected from the level of the shoulder, and tail blastemas amputated at the 12th myotome from the cloaca were collected at the 10th myotome of the regenerating tail. These limb and tail blastemas were immunostained as previously described^{15,25,26}. Briefly, the samples were fixed with MEMFA fixative at 4 °C

overnight, and were rinsed with PBS several times. The buffer was replaced from PBS to 10%, 20% and 30% sucrose (Sigma)/PBS, then the samples were embedded in Tissue-Tek O.C.T. Compound (Sakura) for cryosection and the tissues were sectioned at 10-µm thickness with Microm HM 560 cryostat (Thermo). Primary antibodies used: mouse anti-BrdU (MPI-CBG antibody facility, Bu20a 1/400), rabbit anti-BrdU (antibodies-online, 1/600), mouse anti-PAX7 (MPI-CBG antibody facility, PAX7 1/450), rabbit anti-MEF2 (Santa Cruz, 1/200), rabbit anti-AxMLP-C terminus (1/200), rabbit anti-GFP (Rockland, 1/400), rabbit anti-FITC (Invitrogen, 1/400), mouse anti-FITC (Jackson ImmunoResearch Laboratories, 1/400), rat anti-MBP (GeneTex, 1/200). The following appropriate fluorophore-conjugated secondary antibodies were used (all in 1/200 dilution): donkey anti-mouse Alexa Fluor (AF) 647 (Molecular Probes), goat anti-mouse AF 647 (Jackson ImmunoResearch Laboratories), donkey anti-mouse AF 488 (Molecular Probes), goat anti-rabbit AF 647 (Jackson ImmunoResearch Laboratories), donkey anti-rabbit AF 488 (Molecular Probes), donkey anti-rat AF 488 (Molecular Probes). The cell nuclei were stained with Hoechst 33342 (Sigma, final 0.5 µg ml⁻¹). Imaging for the stained sections was performed with Zeiss Observer.Z1 (Zeiss) controlled by Axiovision software or Zen2 (Zeiss).

qRT-PCR. Total RNA preparation, reverse transcription and qRT-PCR were essentially described in the previous work². Briefly, three biological replicas were prepared for each time point and they were technically independent in all the processes (tissue collection, RNA preparation, cDNA synthesis and qRT-PCR). Eight to approximately ten limb or tail blastemas from one time point were collected in one tube and homogenized by POLYTRON PT1600E (KINEMATICA). Total RNA was purified with RNeasy Mini or Midi Kit (QIAGEN) according to the manufacturer's manual. cDNA was synthesized from 300 ng of total RNA using SuperScript III First-Strand Synthesis System (Invitrogen) and qRT-PCR was performed with Power SYBR Green Master Mix (Invitrogen) in total volume of 12 µl with the final primer concentration of 300 nM on the LightCycler 480 (Roche). To obtain the values of fold change for each time point, the relative concentration of the PCR products was calculated by the standard curve method. To obtain the standard curves of the limb time course or the tail time course respectively, the dilution series (1/4, 1/16, 1/64, 1/256 and 1/1,024) were made from the mixture of cDNAs that were equivalently collected from the cDNA samples in all the different time points. These dilution series were used as the template for the PCR and the relative concentrations were calculated by LightCycler 480 Software (Roche) based on the standard curves. The concentration of AxMlp was normalized with that of Rpl4 (large ribosomal protein 4). Primers used for PCR were showed in Supplementary Table 2 (for AxMlp, oligonucleotides numbers 20, 21; for Rpl4, oligonucleotides numbers 22, 23). The raw values of qPCR data are shown in Supplementary Table 1.

Protein injection into axolotl tail and limb. The dialysed protein samples: purified AxMLP, depleted media (flow-through) (see earlier) or PBS as a negative control were injected into mature (not regenerating) tails with a pressure injector, PV830 Pneumatic Picopump (World Precision Instruments). These protein samples were co-injected with tetramethylrhodamine dextran MW 70,000 (Molecular Probes, final 2.5 mg ml⁻¹) as a tracer. A glass capillary (Harvard Apparatus) for the injection was pulled with P-97 Micropipette Puller (Sutter Instrument) and sharpened manually (external tip diameter: 30 µm). The injection efficiency was confirmed based on the intensity of the rhodamine under the fluorescence dissecting microscope (SZX 16, OLYMPUS). No animals were excluded from the analysis. In total, 270 ng of purified AxMLP or equivalent volume of controls were injected into one side of the tail. Injected animals were kept in clean tap water for 3 days at room temperature. The animals were injected intraperitoneally with 30 µl of 2.5 mg ml⁻¹ BrdU (Sigma) 4 h before collecting the tails (Fig. 2a). The injected part of the tails was identified by rhodamine-positive myotomes and these tails were fixed, embedded, cryosectioned and immunostained as described earlier. For the quantification, the tile images of whole cross-sections of the tails from Zeiss Observer.Z1 (Zeiss) were stitched by Axiovision software (Zeiss). Three sections from five different animals in each condition (PBS, flow-through or purified AxMLP injection, respectively) were taken, and the marker-positive nuclei (BrdU⁺, PAX7⁺, MEF2⁺ or Hoechst⁺) on the sections were counted by hand. The cells in spinal cord, epidermis and notochord were separately counted based on morphology. The label "Other tissues", contained mainly mesenchymal cells and endothelial cells, and was calculated by the subtraction from the total number to the number of all the other specific cell types.

For the protein injection into the limb, the procedure was essentially as described earlier. Purified AxMLP protein was injected into the mature (not regenerating) right lower limbs at the centre between the elbow and the wrist. The control samples (flow-through fraction or PBS) were injected into the left limbs of the same animal that were injected with purified AxMLP on their right limbs. In total 2.0 µg purified AxMLP or equivalent volume of controls were injected into

the limbs. The animals were injected intraperitoneally with 30 µl of 2.5 mg ml⁻¹ BrdU (Sigma) 12 h before collecting the limbs (Extended Data Fig. 4e). For the quantification, at least a total of 1,000 cells per one animal were counted from four different animals in each condition (PBS, flow-through or purified AxMLP injection, respectively), and the marker-positive nuclei (BrdU⁺, PAX7⁺, MEF2⁺, MBP⁺ or Hoechst⁺) on the sections were counted by hand. The cells in epidermis and bone/perichondrium were separately counted with their morphology. The label "Other tissues", contained mainly mesenchymal cells and endothelial cells, and was calculated by the subtraction from the total number to the number of all the other specific cell types.

For the acceleration experiment, purified AxMLP, flow-through or PBS as a negative control were injected into mature (not regenerating) tail as the first (3 days before amputation) injection and as the second (1 day before amputation) injection and injected into the blastema as the third (2 days post-amputation) injection (Extended Data Fig. 10a). These samples were co-injected with tetramethylrhodamine dextran MW 70,000 (Molecular Probes, final 2.5 mg ml⁻¹) as a tracer. The injection efficiency was confirmed based on the intensity of the rhodamine under the fluorescence dissecting microscope (SZX 16, OLYMPUS). No animals were excluded from the analysis. The samples were injected into both side of the tail and in each injection, 600 ng, then, in total 1.8 µg protein or equivalent volume of controls were injected. Injected animals were kept in clean tap water for 4 days at room temperature. The length of the blastema was measured from the amputation plane to the tip at the spinal cord level at 4 dpa based on the stereoscope images (SZX 16, OLYMPUS).

Morpholino electroporation. In vitro assay. A1 myoblasts were transfected with original clone *BL212a101*, *AxMLP-3C-His*, *ΔN-AxMLP-3C-His* or empty pCMV-SPORT6-3C-His plasmids and co-transfected with AxMLP-specific morpholinos (Gene Tools; Supplementary Table 2: oligonucleotides numbers 24, 26) or control morpholinos (Gene Tools; Supplementary Table 2: oligonucleotides numbers 25, 27) using Microporator (Digital Bio) according to the manufacturer's manual with some modifications. All morpholinos were modified with FITC at the 3' end. A1 myoblasts were re-suspended in 1 × Steinberg solution at a density of 5.0 × 10⁶ cells per ml followed by incubation of 10 µl cell suspension with 0.5 µg of plasmid and 1 µl of the morpholino (final 100 µM in the incubation). Electroporation was performed at 1,000 V, 35 mS pulse length and 3 pulses and the electroporated cells were spread in 10% FCS AMEM media²⁴ on a 24-well plate (Nunc), immediately after the electroporation. The culture medium was replaced by new media at 24 h post-electroporation and the cells were kept in culture at 72 h post-electroporation. The electroporated cells were fixed with 1.5% PFA/PBS, and the cell lysates were prepared for western blotting. Primary antibodies used for immunostaining: mouse anti-His (QIAGEN, 1/200), mouse anti-FITC (Jackson ImmunoResearch Laboratories, 1/400), rabbit anti-FITC (Invitrogen, 1/400), rabbit anti-AxMLP-full length (1/1,000). Secondary antibodies used for immunostaining (all in 1/250 dilution): goat anti-mouse Cy3 (Jackson ImmunoResearch Laboratories), goat anti-mouse AF488 (Jackson ImmunoResearch Laboratories), donkey anti-rabbit AF 488 (Molecular Probes), goat anti-rabbit Cy3 (Jackson ImmunoResearch Laboratories). Images of the stained cells were taken with Zeiss Observer.Z1 (Zeiss) controlled by Axiovision software (Zeiss).

In vivo assay with rescue protein injection. Electroporation to the spinal cord was performed as previously described with some modifications²⁷. To deliver morpholino into the spinal cord and both sides of the tail epidermis, the tail required electroporation twice with NEPA 21 electroporator (Nepa Gene). The first electroporation was for the spinal cord and one side (left) of the epidermis, and the second electroporation was for the other side (right) of the epidermis. 1.5 µl of morpholino (1.0 mM) was loaded onto a small piece of tissue paper on the left side of the epidermis. Approximately 3 µl of morpholino (1.0 mM) was injected into the spinal cord and immediately electroporated (first electroporation). Sequentially, 1.5 µl of morpholino (1.0 mM) was loaded onto a small piece of tissue paper on the right side of the epidermis and electroporated (second electroporation). The first electroporation conditions: poring pulse, 70 V, 5.0 mS pulse length and 1 pulse; transfer pulse, 55 V, 55 mS pulse length, 5 pulses and 15% decay. The second electroporation conditions: poring pulse, 70 V, 10 mS pulse length and 1 pulse; transfer pulse, 30 V, 30 mS pulse length, 7 pulses and 5% decay. FITC dextran MW 70,000 (Molecular Probes, final 5 mg ml⁻¹) was used as a negative control, since morpholinos were labelled with FITC. The electroporation efficiency in the spinal cord and epidermis was examined based on the intensity of the FITC under the fluorescence dissecting microscope (SZX 16, OLYMPUS). The animals with low FITC intensity were excluded from the next step of the experiments. Three days post-electroporation, the tails were amputated at the level of the maximal morpholino electroporated part. One day post-amputation, a total of 360 ng (180 ng for the spinal cord and 180 ng for blastema) of purified AxMLP or

equivalent volume of control flow-through fraction was injected into the spinal cord and the blastema to rescue the morpholino effect. The length of the blastema was measured from the amputation plane to the tip at the spinal cord level on 1, 3, 6, 10 and 14 dpa based on the stereoscope images (SZX 16, OLYMPUS). To detect BrdU incorporation, the animals were injected intraperitoneally with 30 µl of 2.5 mg ml⁻¹ BrdU (Sigma) 4 h before collecting the tails at 3 dpa. Fixation, embedding, cryosection, staining and imaging were described earlier. For the quantification, 3 cross-sections of the blastema (200–300 µm posterior to the amputation plane) from four different animals in each condition (FITC/flow-through, FITC/purified AxMLP, control morpholino/flow-through, control morpholino/purified AxMLP, AxMLP-specific morpholino/flow-through, AxMLP-specific morpholino/purified AxMLP, respectively) were taken, and the marker-positive nuclei (BrdU⁺, PAX7⁺, MEF2⁺ or Hoechst⁺) on the sections were counted by hand.

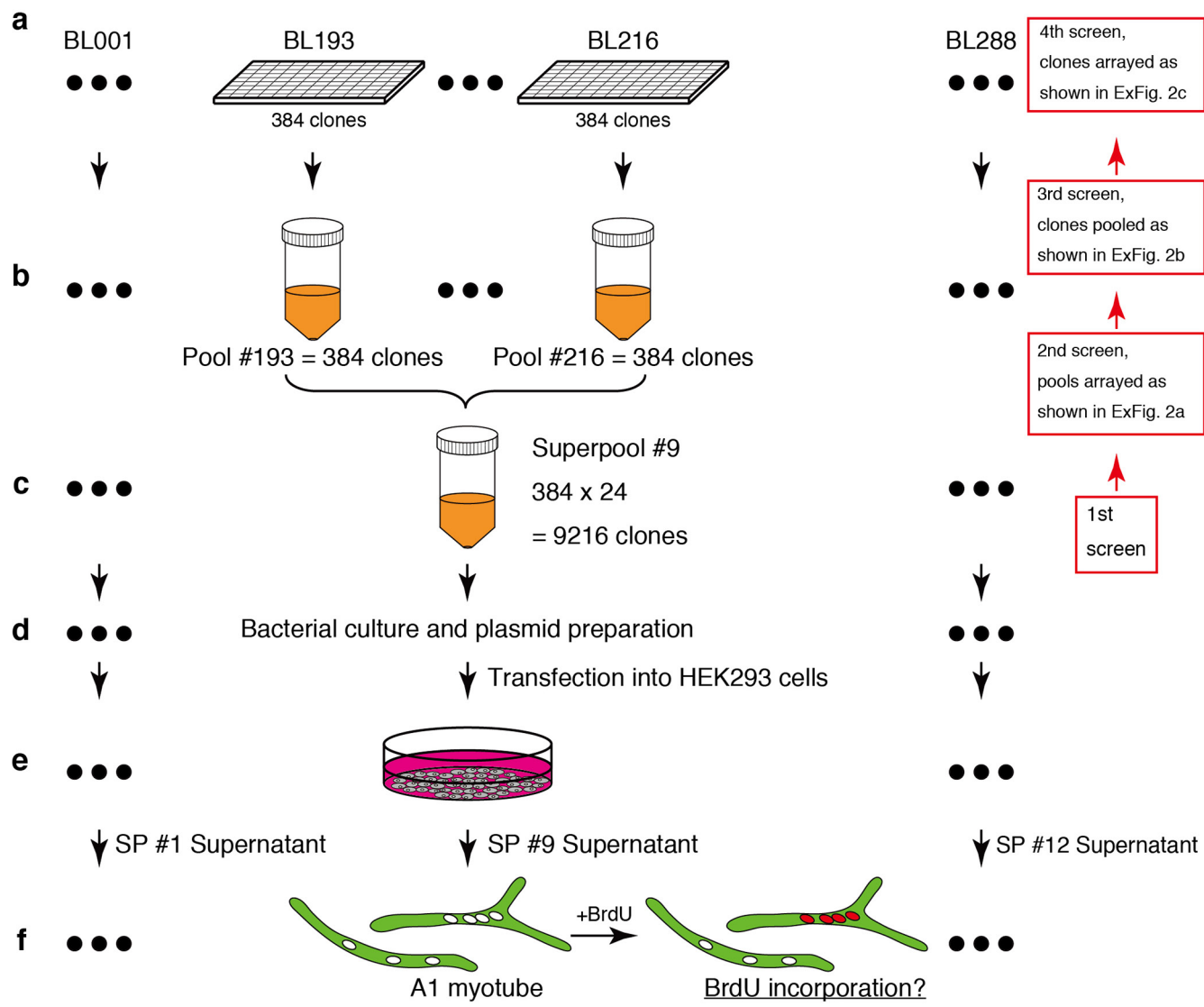
Newt experiments. Animals. Red-spotted newts, *Notophthalmus viridescens*, were supplied by Charles D. Sullivan Co. Animals were anaesthetized in 0.1% ethyl 3-aminobenzoate methanesulfonate (Sigma) for 15 min. Forelimbs were amputated above the elbow, and the bone and soft tissue were trimmed to produce a flat amputation surface. Animals were left to recover overnight in an aqueous solution of 0.5% sulfamerazine (Sigma). At specified time points, the uninjured or regenerating limbs were collected. All surgical procedures were performed according to the European Community and local ethics committee guidelines.

Protein injection and cell cycle assays in newt limbs. The general condition in the newt experiments: 2 µl of 5 mg ml⁻¹ purified AxMLP protein or equivalent volume of flow-through (AxMLP depleted fraction) was injected into the newt limbs. For EdU labelling, animals were injected intraperitoneally with 50–100 µl of 1 mg ml⁻¹ EdU. To investigate the effect of AxMLP on intact newt limbs, purified AxMLP or flow-through was injected into the uninjured limb twice at day 1 and day 3. EdU was administered daily from day 1 to day 5 (Fig. 3a, top). To investigate the effect of AxMLP on regenerating limbs, purified AxMLP or flow-through was injected into the regenerating limbs at 7 and 10 dpa (Fig. 3b, top). EdU was administered daily from 8 to 13 dpa. For labelling myofibre progeny, a *H2B-YFP* reporter construct was introduced into myofibres before amputation as previously described¹⁵ (Fig. 3c, top). Cell cycle re-entry was quantified by EdU incorporation in the YFP⁺ myofibre progeny at 13 dpa.

Immunohistochemistry. Frozen sections (5–10 µm) were thawed at room temperature and fixed in 4% formaldehyde for 5 min. Sections were blocked with 5% donkey serum and 0.1% Triton-X for 30 min at room temperature. Sections were incubated with anti-GFP (Abcam 6673), anti-PAX7 (DSHB) or anti-MHC (DSHB) overnight at 4 °C and with secondary antibodies for 1 h at room temperature. Antibodies were diluted in blocking buffer and sections were mounted in mounting medium (DakoCytomation) containing 5 µg ml⁻¹ DAPI (Sigma). EdU detection was performed as previously described¹⁵. An LSM 700 Meta laser microscope with LSM 6.0 Image Browser software (Carl Zeiss) was used for confocal analyses. One in every eight sections was selected and labelled. For PAX7⁺ satellite cell counting, three sections were randomly selected and counted. For blastema YFP⁺ cell counting, all the sections in the region from regenerate tip to the bone were counted.

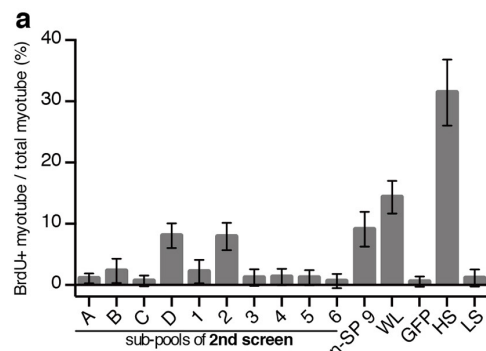
Statistical analysis. Statistical analyses were performed using GraphPad Prism 6.0 (GraphPad Software). Student's *t*-test, parametric, two-tail testing was applied to populations to determine the *P* values indicated in the figures. Significance was considered to have been reached at *P* values from <0.05. No statistical methods were used to predetermine sample size. *In vivo* axolotl experiments were not randomized and no blind tests were applied.

20. Kragl, M. et al. Cells keep a memory of their tissue origin during axolotl limb regeneration. *Nature* **460**, 60–65 (2009).
21. Sive, H. L., Grainger, R. M. & Harland, R. M. *Early Development of Xenopus laevis: A Laboratory Manual* (Cold Spring Harbor Laboratory, 2000).
22. Habermann, B. et al. An *Ambystoma mexicanum* EST sequencing project: analysis of 17,352 expressed sequence tags from embryonic and regenerating blastema cDNA libraries. *Genome Biol.* **5**, R67 (2004).
23. Ferretti, P. & Brookes, J. P. Culture of newt cells from different tissues and their expression of a regeneration-associated antigen. *J. Exp. Zool.* **247**, 77–91 (1988).
24. Lo, D. C., Allen, F. & Brookes, J. P. Reversal of muscle differentiation during urodele limb regeneration. *Proc. Natl. Acad. Sci. USA* **90**, 7230–7234 (1993).
25. Roensch, K., Tazaki, A., Chara, O. & Tanaka, E. M. Progressive specification rather than intercalation of segments during limb regeneration. *Science* **342**, 1375–1379 (2013).
26. Zarzosa, A. et al. Axolotls with an under- or oversupply of neural crest can regulate the sizes of their dorsal root ganglia to normal levels. *Dev. Biol.* **394**, 65–82 (2014).
27. Rodrigo-Albors, A. & Tanaka, E. M. in *Salamanders in Regeneration Research: Methods and Protocols* (eds Kumar, A. & Simon, A.) 115–126 (Springer, 2015).

6-day tail blastema cDNA library: $384 \times 288 = 110,592$ clones

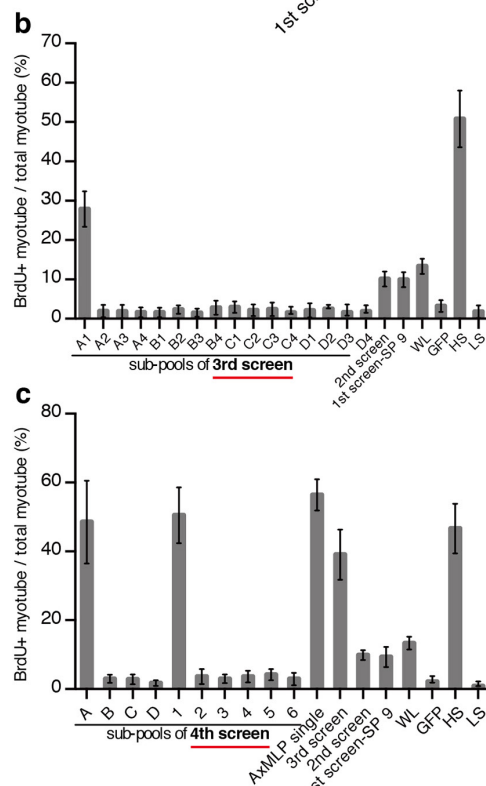
Extended Data Figure 1 | Schematic illustration of the expression cloning approach. **a**, 110,592 clones from a 6-day tail blastema library were arrayed on 288×384 -well plates. **b**, One 384-well plate was pooled into one conical tube and called a ‘pool’. In total, 288 pools were prepared from the library. **c**, Twenty-four pools were combined in one conical tube and called a ‘superpool’ (SP) containing 9,216 clones. In total 12 superpools were prepared. **d**, Bacteria of each superpool was cultured

and plasmid was prepared. **e**, The superpool plasmids were transfected into HEK293 cells. **f**, Individual supernatants were tested on A1 myotubes for cell cycle re-entry activity (myotube assay) (see Fig. 1b). Positive superpools were successively subfractionated and the assay process was repeated back from the positive superpool (first screen) to come to a single clone (fourth screen) (**a–c**, right) (see Extended Data Fig. 2a–c).



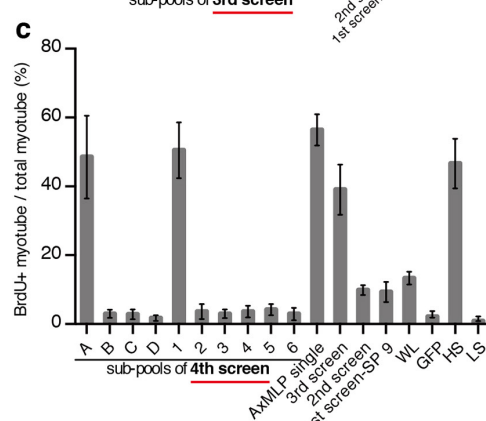
Map of pooled "Pool"

	Pools in Sub-pool 1	Pools in Sub-pool 2	Pools in Sub-pool 3	Pools in Sub-pool 4	Pools in Sub-pool 5	Pools in Sub-pool 6
Pools in Sub-pool A	p193	p194	p195	p196	p197	p198
Pool in Sub-pool B	p199	p200	p201	p202	p203	p204
Pools in Sub-pool C	p205	p206	p207	p208	p209	p210
Pools in Sub-pool D	p211	p212	p213	p214	p215	p216



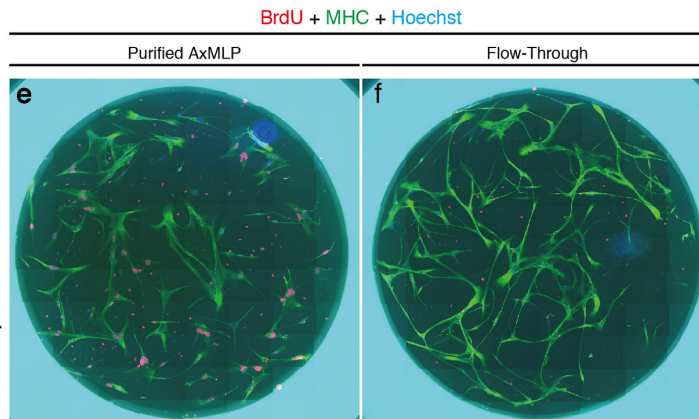
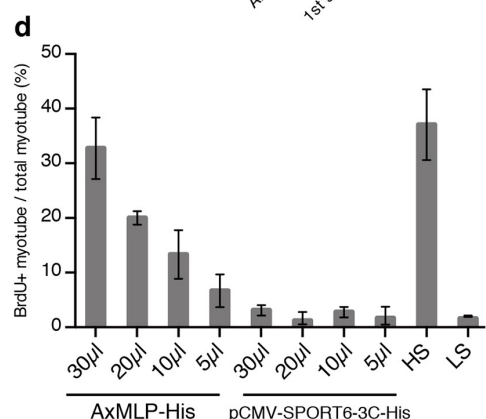
Map of pooled "clones"

BL212 (384 clones)	Group A (96 clones)	Sub-pool A1 (24 clones)
	Group B (96 clones)	Sub-pool A2 (24 clones) Sub-pool A3 (24 clones) Sub-pool A4 (24 clones)
	Group C (96 clones)	Sub-pool B1 (24 clones) Sub-pool B2 (24 clones) Sub-pool B3 (24 clones) Sub-pool B4 (24 clones)
	Group D (96 clones)	Sub-pool C1 (24 clones) Sub-pool C2 (24 clones) Sub-pool C3 (24 clones) Sub-pool C4 (24 clones)
		Sub-pool D1 (24 clones) Sub-pool D2 (24 clones) Sub-pool D3 (24 clones) Sub-pool D4 (24 clones)



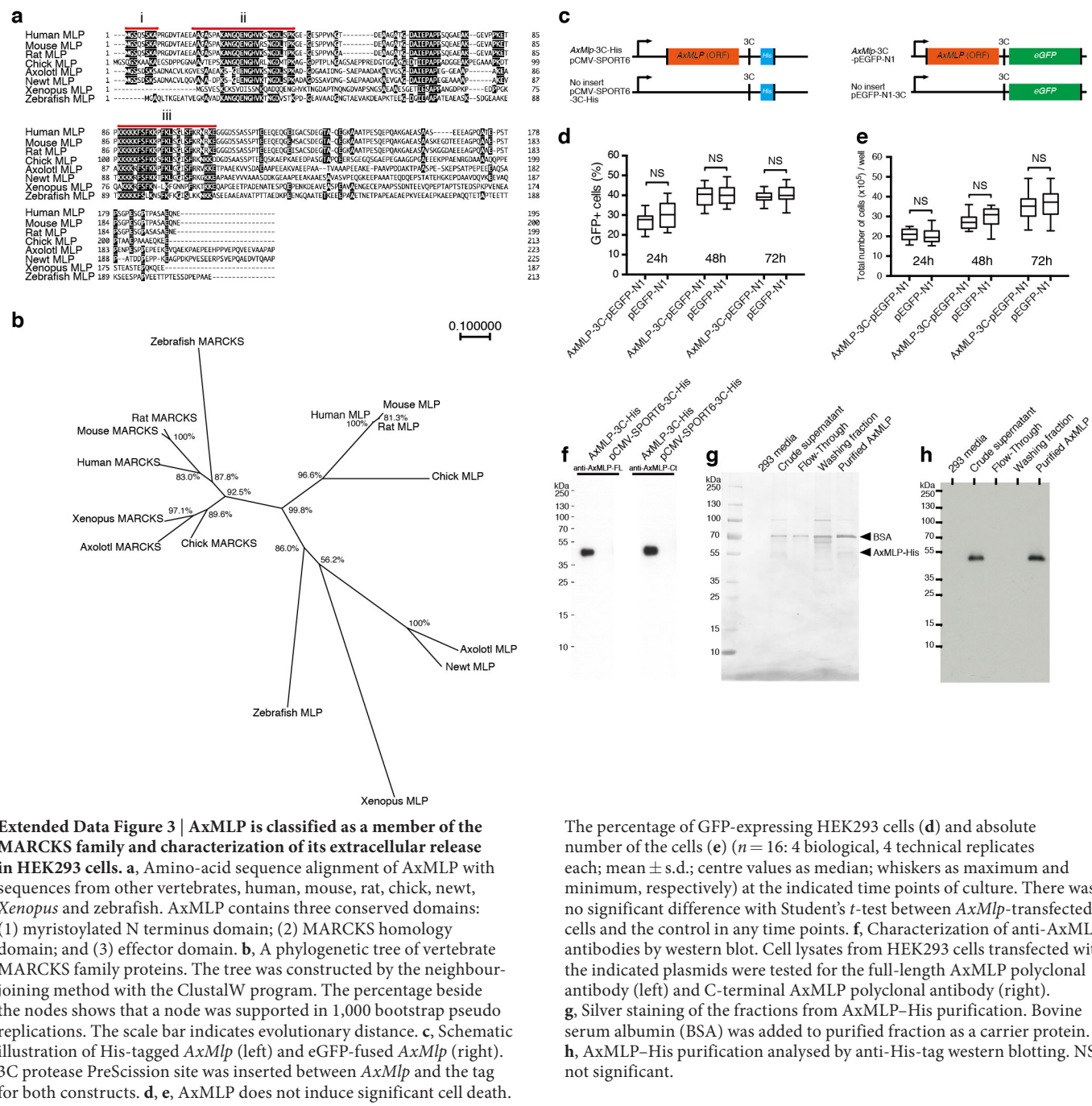
Map of pooled "clones"

	Clones in Sub-pool 1	Clones in Sub-pool 2	Clones in Sub-pool 3	Clones in Sub-pool 4	Clones in Sub-pool 5	Clones in Sub-pool 6
Clones in Sub-pool A	c1	c2	c3	c4	c5	c6
Clones in Sub-pool B	c7	c8	c9	c10	c11	c12
Clones in Sub-pool C	c13	c14	c15	c16	c17	c18
Clones in Sub-pool D	c19	c20	c21	c22	c23	c24

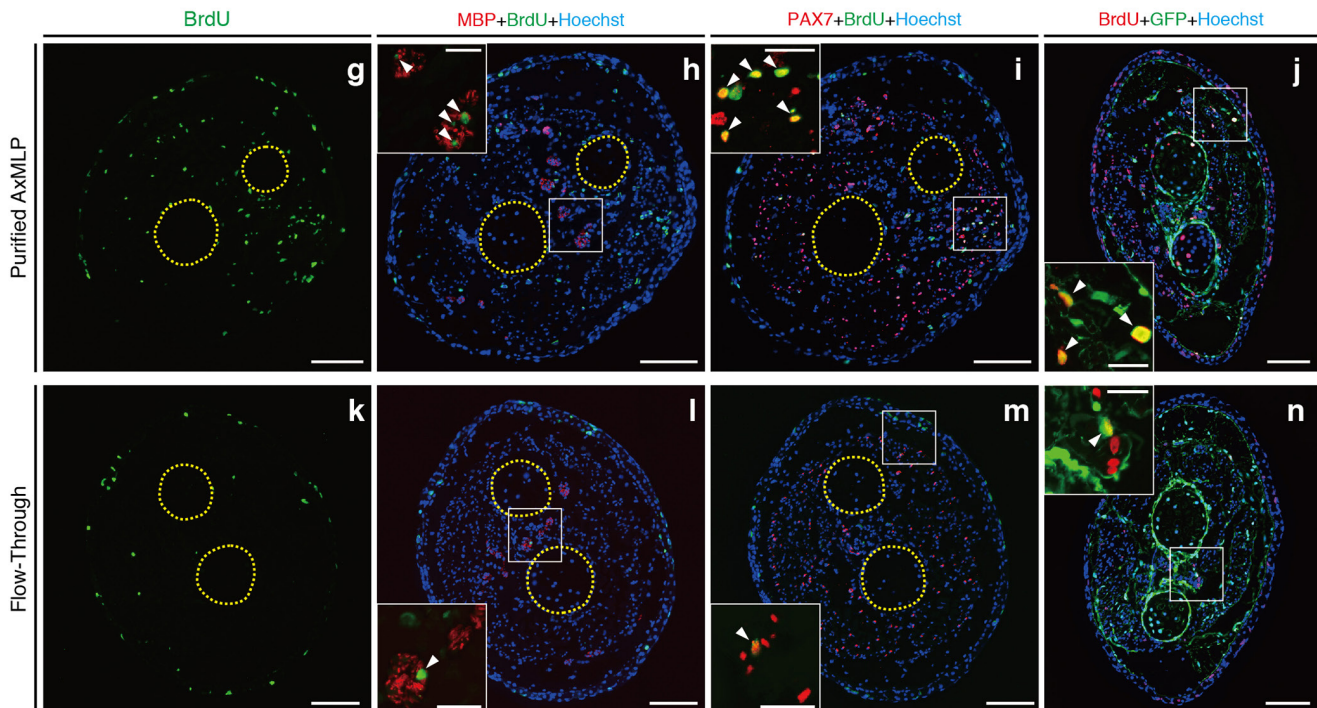
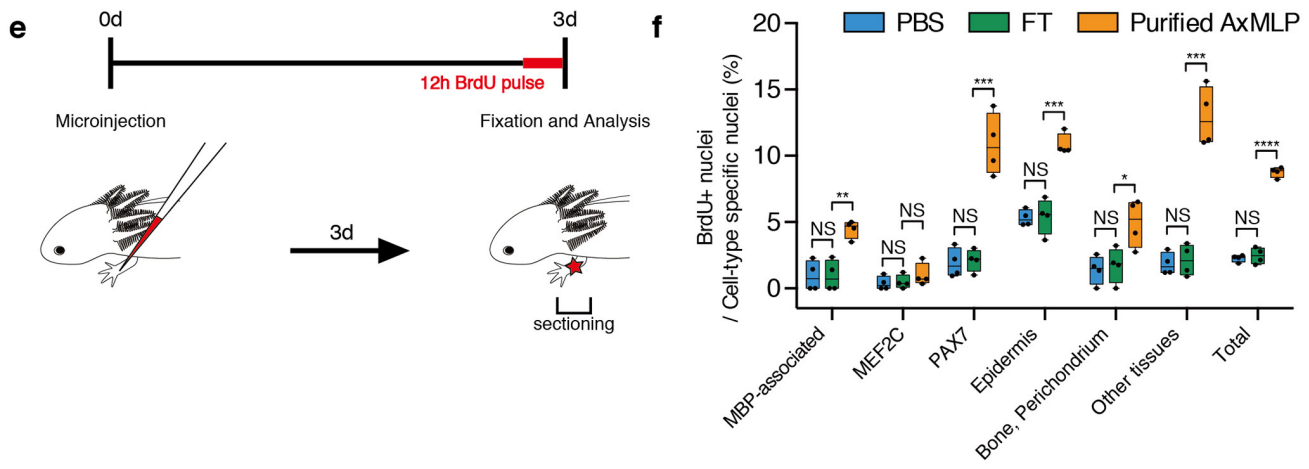
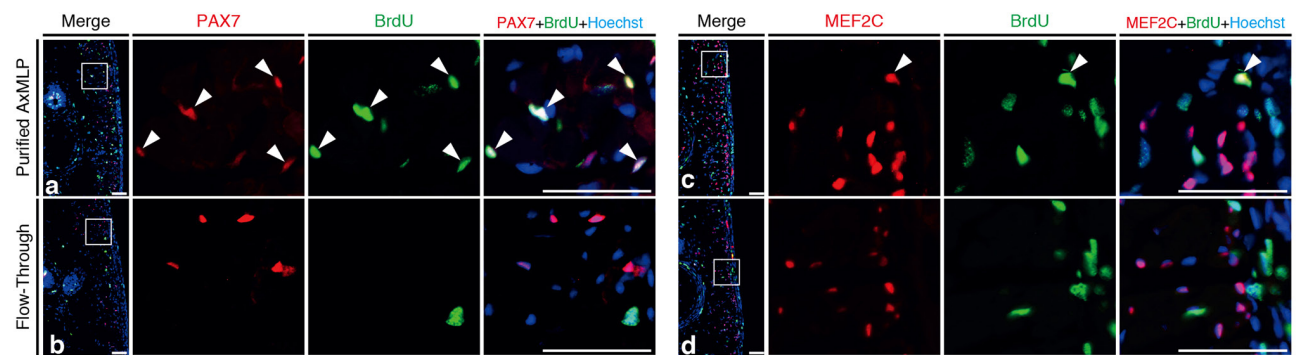


Extended Data Figure 2 | Expression cloning of AxMLP as a myotube cell cycle inducer. **a**, The results of the second-round screen of superpool 9 (see Fig. 1b and Extended Data Fig. 1) and its sub-pooling diagram (right). Sub-pool D and sub-pool 2 showed higher BrdU incorporation activity than the others, identifying pool number 212 as positive ($n = 12$: 4 biological, 3 technical replicates each; mean \pm s.d.). **b**, The result of the third-round screen of pool number 212 from superpool 9 and its sub-pooling diagram (right). Sub-pool A1 showed activity ($n = 6$: 2 biological, 3 technical replicates each; mean \pm s.d.). **c**, Fourth-round screen of SP9 identified a single active clone (c1), AxMlp ($n = 12$: 4 biological, 3 technical replicates each; mean \pm s.d.). The pooling diagram is shown

on the right side. **d**, AxMLP supernatant induces an S-phase response in a dose-dependent manner in the newt myotube assay. Different amounts of AxMLP-containing supernatant (30 µl, 20 µl, 10 µl and 5.0 µl, respectively) were provided to the myotube cell culture medium. The myotube BrdU incorporation correlated with the amount of supernatant provided, whereas pCMV-SPORT6 supernatant did not provoke cell cycle entry at any dose ($n = 6$: 2 biological, 3 technical replicates each; mean \pm s.d.). **e, f**, Newt myotubes treated with purified AxMLP (e) or flow-through (f) were immunostained for BrdU and MHC. More BrdU-incorporated nuclei (red) in myotubes (green) were observed in culture supplied with purified AxMLP compared with flow-through-treated cultures. Scale bar, 1 mm.

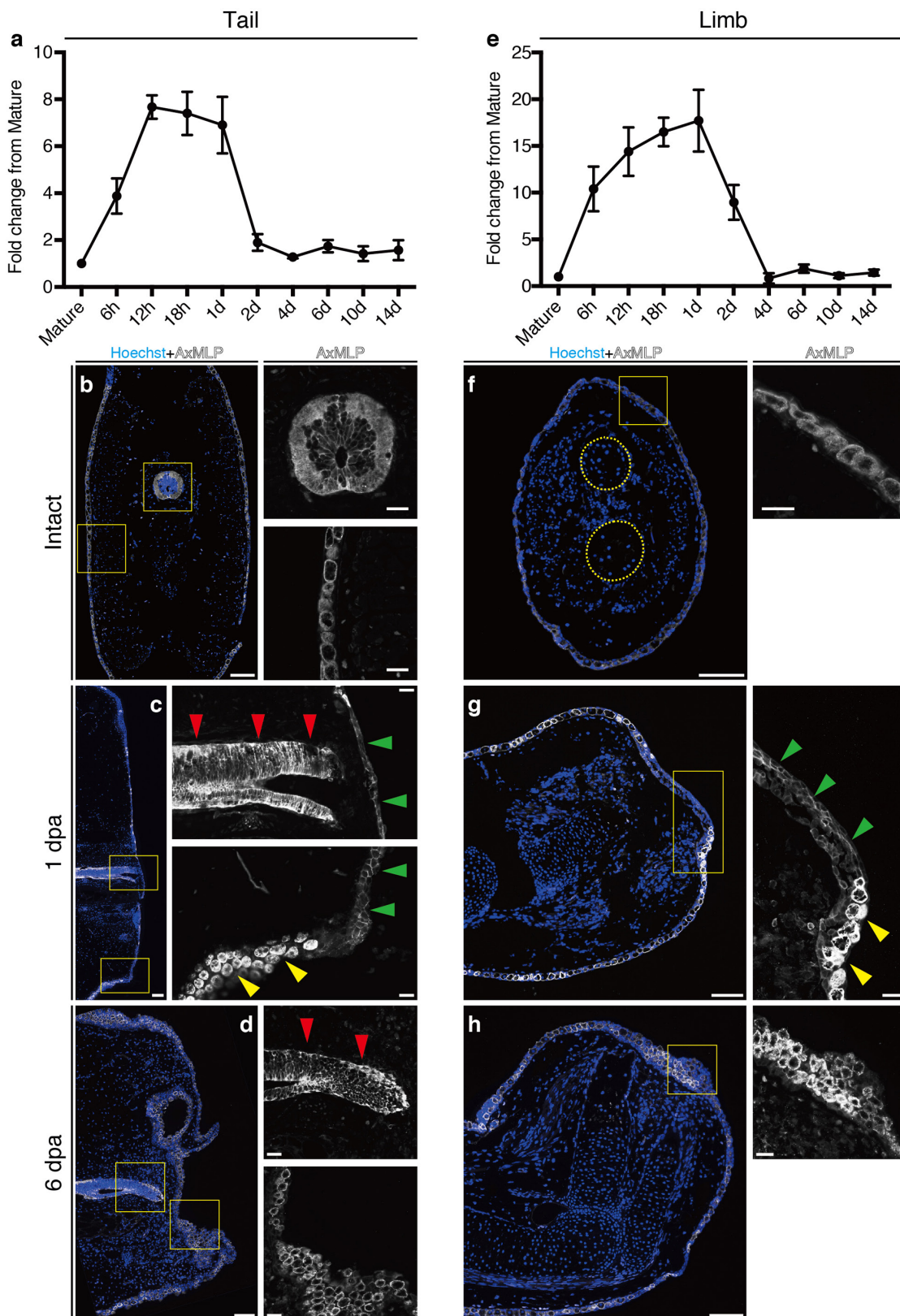


Extended Data Figure 3 | AxMLP is classified as a member of the MARCKS family and characterization of its extracellular release in HEK293 cells. a, Amino-acid sequence alignment of AxMLP with sequences from other vertebrates, human, mouse, rat, chick, newt, *Xenopus* and zebrafish. AxMLP contains three conserved domains: (1) myristoylated N terminus domain; (2) MARCKS homology domain; and (3) effector domain. b, A phylogenetic tree of vertebrate MARCKS family proteins. The tree was constructed by the neighbour-joining method with the ClustalW program. The percentage beside the nodes shows that a node was supported in 1,000 bootstrap pseudo replications. The scale bar indicates evolutionary distance. c, Schematic illustration of His-tagged *AxMlp* (left) and eGFP-fused *AxMlp* (right). 3C protease PreScission site was inserted between *AxMlp* and the tag for both constructs. d, e, AxMLP does not induce significant cell death.



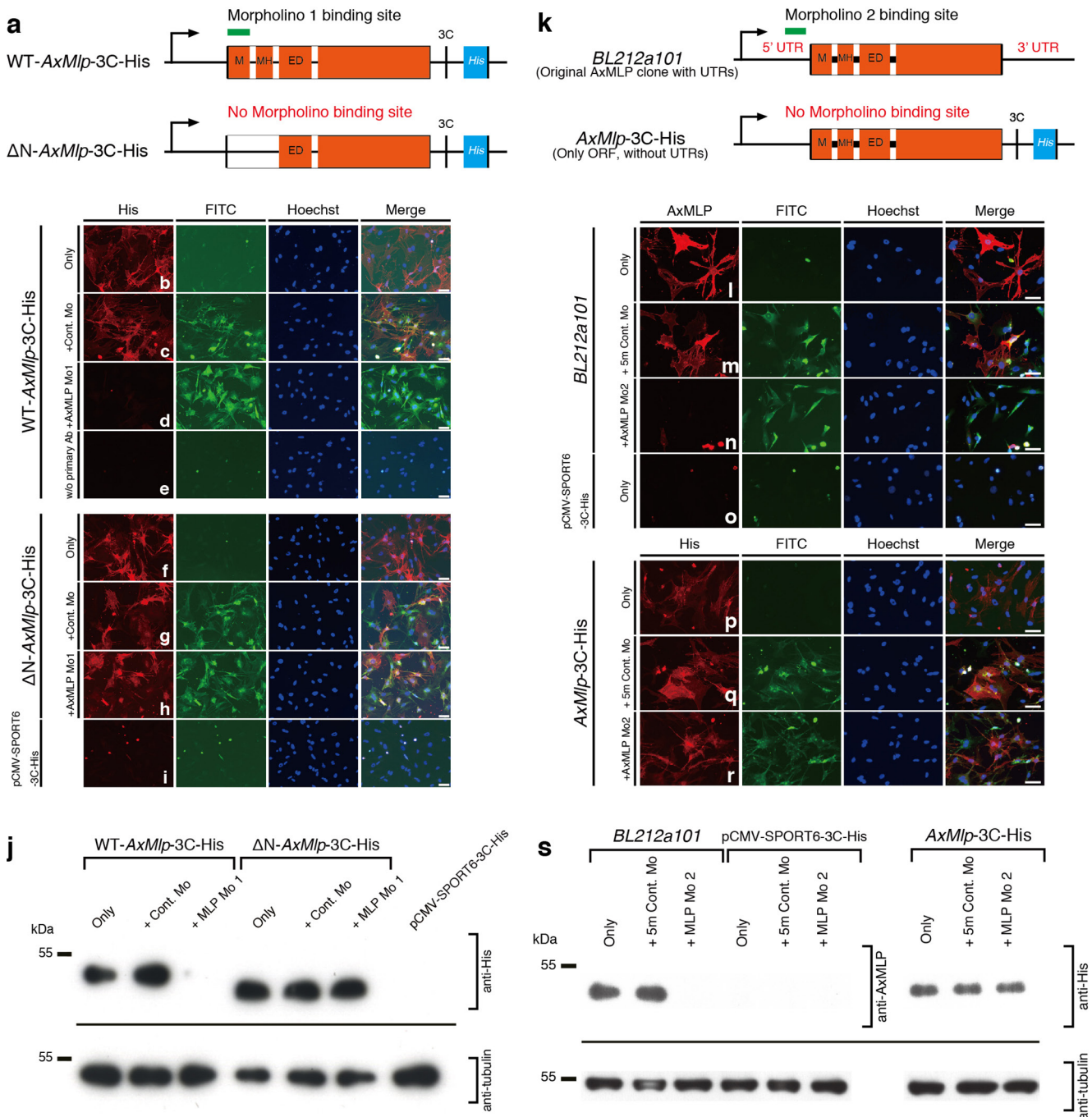
Extended Data Figure 4 | AxMLP is sufficient to induce cell cycle entry in axolotl tail and limb. **a–d**, Sections from AxMLP-injected tails immunostained for BrdU/PAX7 (**a, b**) and BrdU/MEF2C (**c, d**) (refers to data in Fig. 2). Scale bars, 100 μ m. **e**, Schematic illustration of the protein injection into axolotl limb. **f**, Quantification of BrdU⁺ cells in the limbs injected with PBS, flow-through or purified AxMLP ($n = 4$; biological replicates; centre values as median; points represent each sample). **g–n**, Transverse sections from purified AxMLP-injected (**g–j**) or flow-through-injected limbs (**k–n**). Scale bars: lower-magnification images, 200 μ m; higher-magnification images, 50 μ m. Sections were

immunostained for BrdU (**g, k**), BrdU/myelin basic protein (MBP) (**h, l**), BrdU/PAX7 (**i, m**) and BrdU/GFP (**j, n**). GFP⁺ cells represent connective tissues in lateral plate mesoderm (LPM)-GFP transplanted axolotls. All molecular markers used except MBP had nuclear expression, and therefore allowed one-to-one colocalization of nuclear BrdU with nuclear staining of the marker. Therefore, we refer to the MBP data as ‘MBP-associated’. White boxes highlight the magnified images. Yellow circles indicate two bones in the lower limb. NS, not significant; * $P < 0.05$, ** $P < 0.005$, *** $P < 0.0005$, **** $P < 0.00005$ with Student’s *t*-test. White arrowheads indicate marker⁺/BrdU⁺ cells.



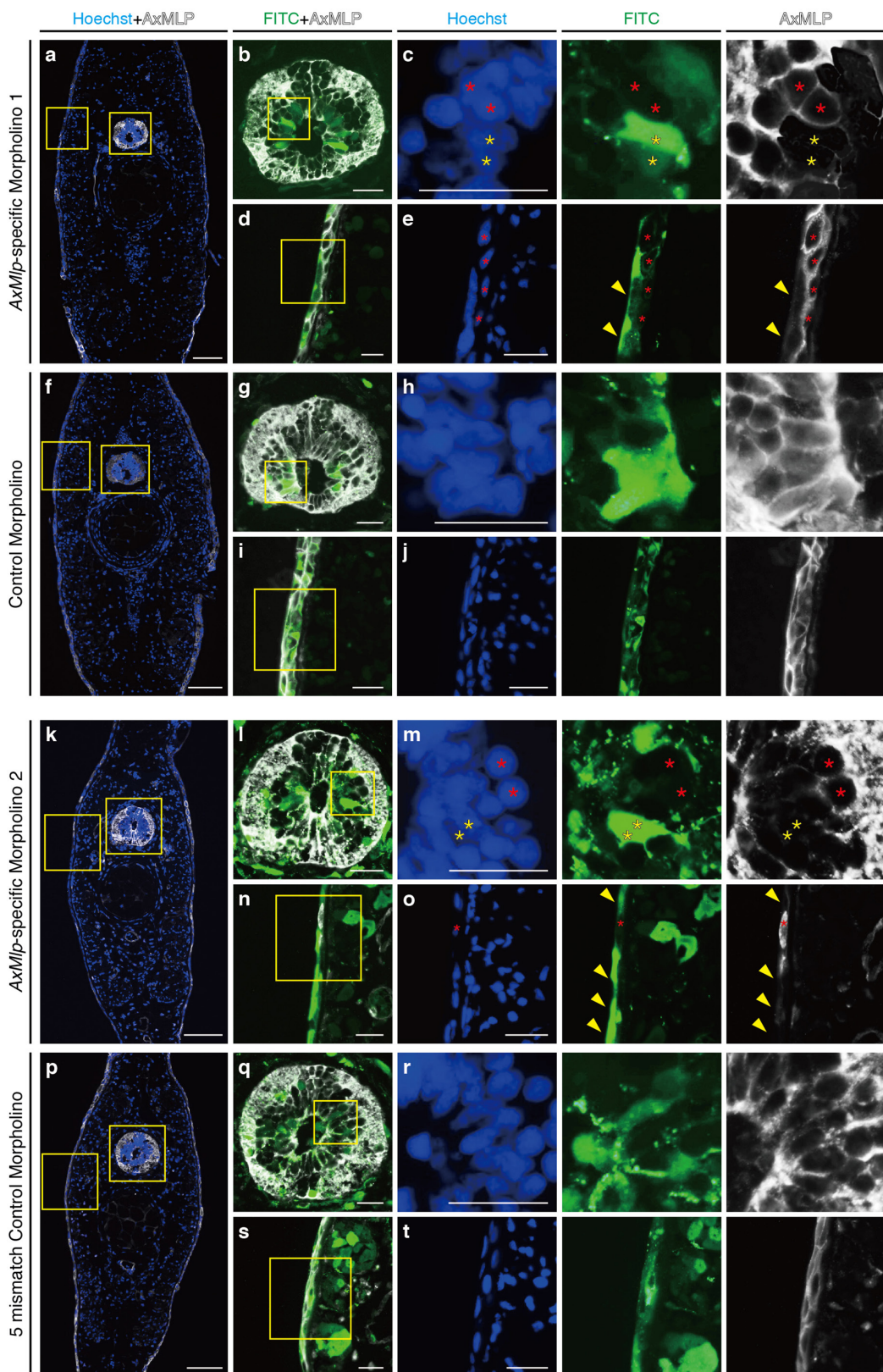
Extended Data Figure 5 | Upregulation of *AxMlp* transcript during early regeneration and alteration of *AxMlp* protein localization in wound epidermis cells. **a, e**, Measurement of *AxMlp* expression by qPCR at the indicated time points during tail (**a**) and limb (**e**) regeneration ($n = 3$: biological replicates; mean \pm s.d.). To obtain the values of fold-change for each time point, the relative concentrations of the PCR products were calculated by the standard curve method. The concentration of *AxMlp* was normalized to that of large ribosomal protein

4 (*Rpl4*). **b-h**, Immunostaining with anti-*AxMlp* antibody (white) on tails (**b-d**) and limbs (**f-h**) of intact (**b, f**; transverse sections), 1 dpa (**c**; sagittal; **g**; horizontal) and 6 dpa (**d**; sagittal; **h**; horizontal) samples. By 6 dpa, the epithelial organization and *AxMlp* expression appeared to be returning to a less tightly adherent, less membrane-associated appearance (**d, h**). Scale bars: left, 200 μ m; right 50 μ m. Red arrowheads indicate spinal cord; green arrowheads indicate wound epidermis; yellow arrowheads indicate normal epidermis; yellow circles indicate two bones in the lower limb.



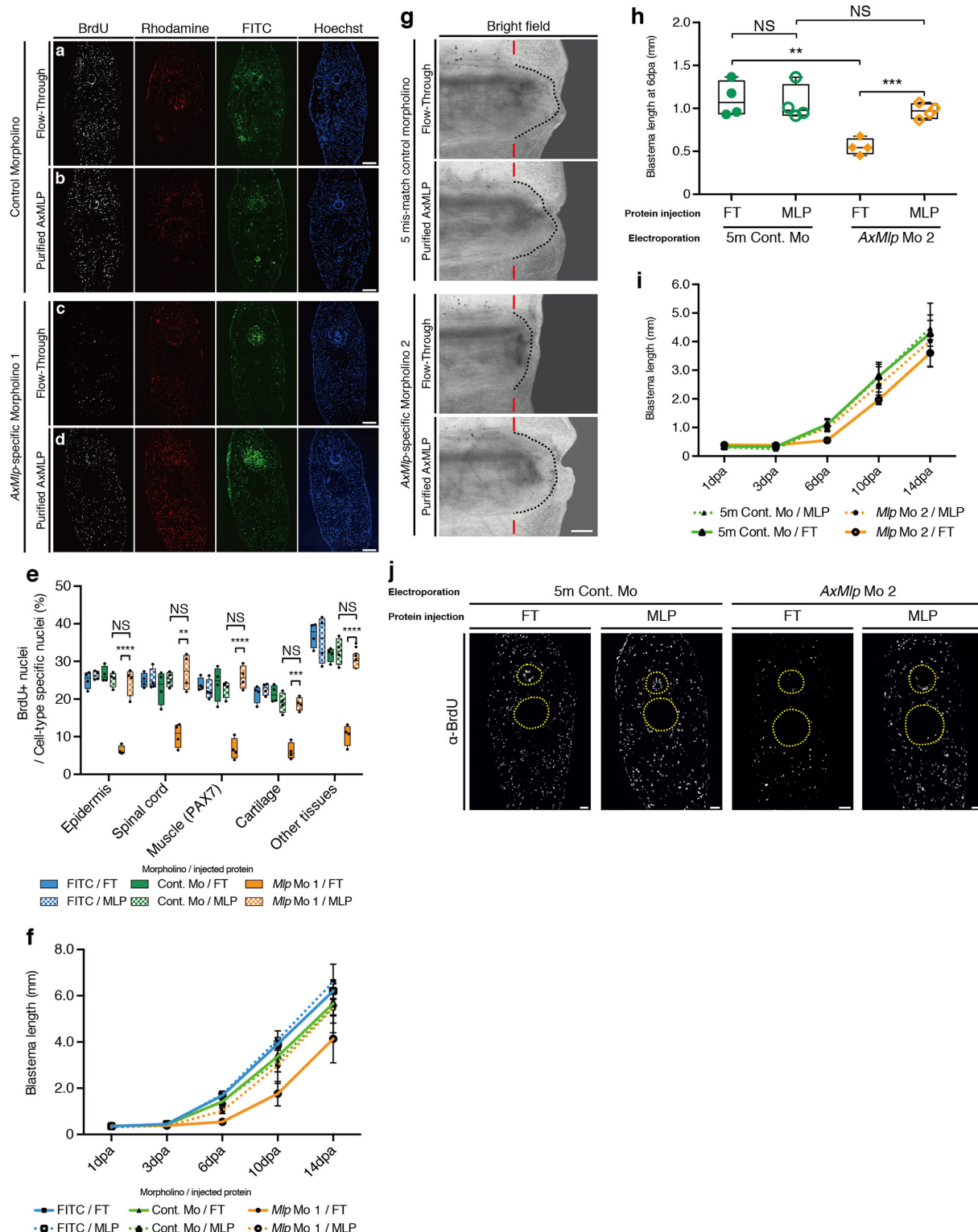
Extended Data Figure 6 | AxMlp morpholinos specifically and efficiently reduce AxMlp translation in cultured cells. **a**, Schematic illustration of wild-type (WT) *AxMlp* (top) and N-terminal deletion *AxMlp* (bottom) constructs used to characterize *AxMlp* morpholino 1. The N-terminally deleted *AxMlp* lacks the morpholino-binding site. Both constructs have a His-tag on their C terminus (**a**). ED, effector domain; M, myristoylated N terminus domain; MH, MARCKS homology domain. **b–e**, Electroporated A1 myoblasts were stained with the indicated markers. **b–e**, Wild-type *AxMlp* plasmid was co-electroporated with the control morpholino (**c**) or the *AxMlp*-specific morpholino 1 (**d**), whereas wild-type *AxMlp* plasmid only (**b**) or wild-type *AxMlp* only without any primary antibody staining were used as negative controls (**e**). **f–h**, Δ N-*AxMlp* plasmid was co-electroporated with the control morpholino (**g**) or the *AxMlp*-specific morpholino 1 (**h**), whereas Δ N-*AxMlp* plasmid only (**f**) or pCMV-SPORT6-3C-His (empty vector) plasmid only served as negative controls (**i**). **j**, Western blotting for the cell lysates from the experiment above. AxMlp morpholino 1 specifically reduced AxMlp protein expression. **k**, Schematic illustration of the

constructs used to characterize *AxMlp* morpholino 2. The original *AxMlp* expression clone from the cDNA library (*BL212a101*; top) was used as it included the 5' untranslated region (UTR) target site for *AxMlp* morpholino 2. The subcloned *AxMlp*-His construct lacks the binding site for *AxMlp* morpholino 2 and was used as the control construct. **l–r**, Electroporated A1 myoblasts were stained with the indicated markers. **l–n**, *BL212a101* plasmid was co-electroporated with the five-mismatch control morpholino (**m**) or the *AxMlp*-specific morpholino 2 (**n**), or *BL212a101* plasmid only (**l**) or pCMV-SPORT6-3C-His (empty vector) plasmid only served as negative controls (**o**). AxMlp was detected using an anti-*AxMlp* antibody (red), and morpholinos were detected via FITC conjugation (green). **p–r**, *AxMlp*-3C-His plasmid was co-electroporated with the five-mismatch control morpholino (**q**) or the *AxMlp*-specific morpholino 2 (**r**) or *AxMlp*-3C-His plasmid only (**p**). AxMlp was detected using an anti-His-tag antibody (red), and morpholinos were detected via FITC conjugation (green). **s**, Western blotting for the cell lysates from the experiment above. *AxMlp* morpholino 2 specifically reduced AxMlp protein expression. Scale bars, 100 μ m.



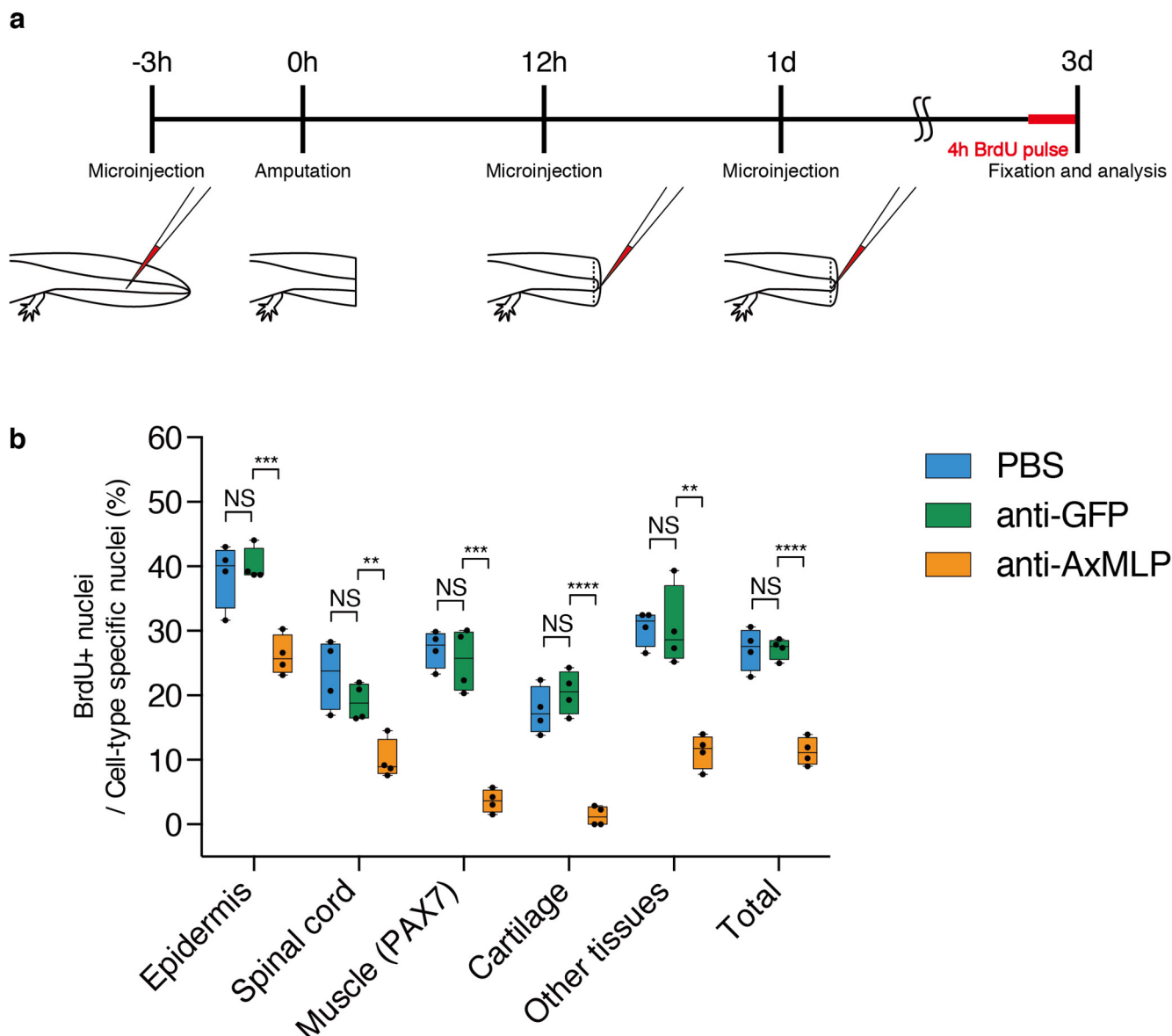
Extended Data Figure 7 | AxMLP morpholinos knockdown endogenous AxMLP *in vivo*. **a–j.** The morpholinos shown in were used in Fig. 4 and Extended Data Figs 6a–j, 8a–f. **k–t.** The morpholinos shown were used in Extended Data Figs 6k–s, 8g–j. Transverse sections from *AxMLP*-specific morpholino 1 (**a–e**) or control morpholino (**f–j**) electroporated tail. **b,** The spinal cord (SC) boxed in **a.** **c,** The higher-magnification images of the spinal cord boxed in **b.** AxMLP expression was detected in morpholino-negative cells (red asterisks), whereas it was reduced in morpholino-positive cells (yellow arrowheads). **d,** The epidermis

boxed in **a, e**, AxMLP expression was unaffected in morpholino-negative cells (red asterisks), whereas it was reduced in morpholino-positive cells (yellow arrowheads). In the control morpholino-electroporated tail (**f**) there was no morpholino-specific knockdown phenotype in either spinal cord (**g, h**) or epidermis (**i, j**). The same experiments were performed with *AxMLP*-specific morpholino 2 (**k–o**) and the corresponding five-mismatch control morpholino (**p–t**). **k–t,** The data sets were the same as **a–j**. Scale bars, 200 μm (**a, f, k, p**); 50 μm (**b–e, g–j, l–o, q–t**).

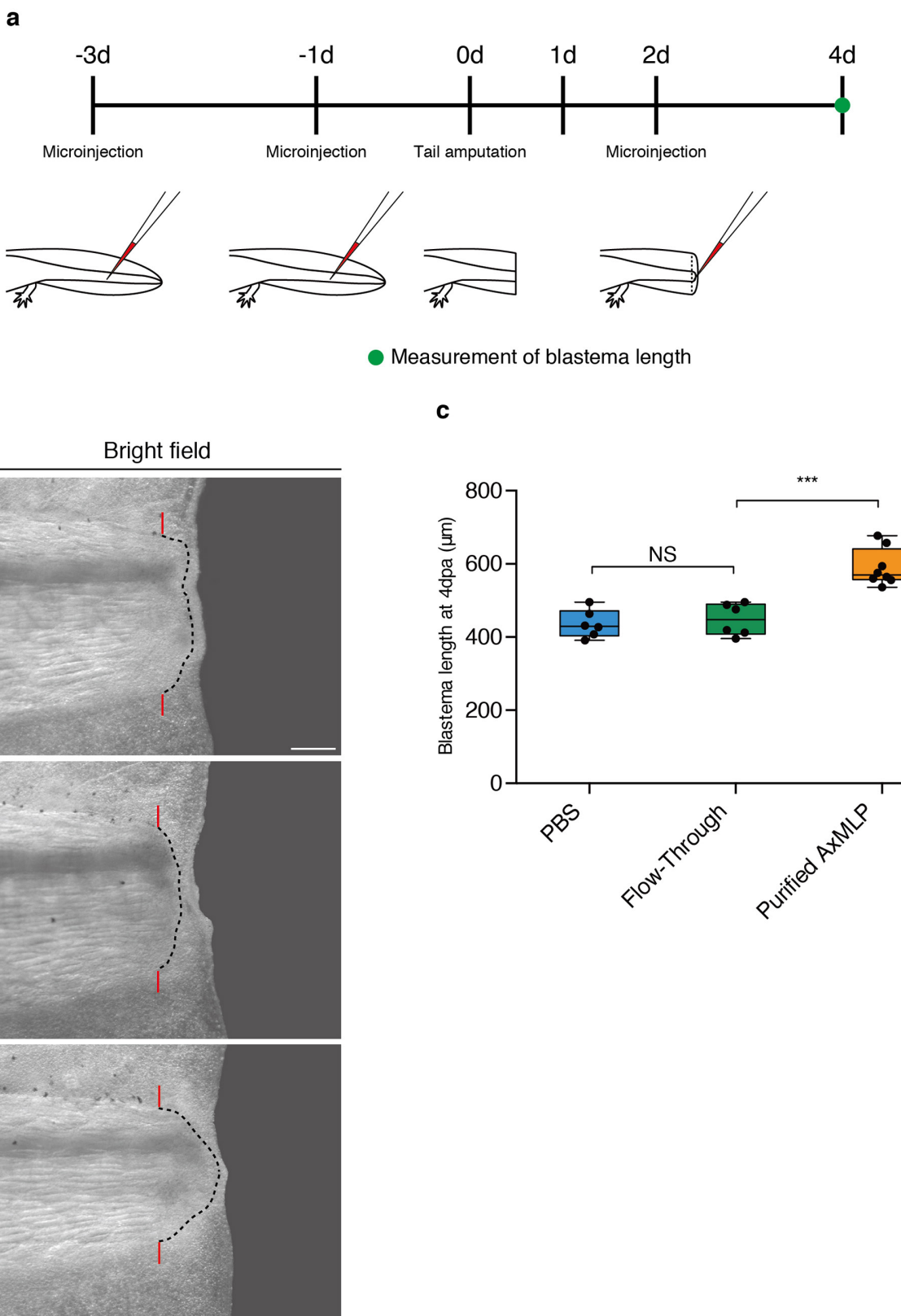


Extended Data Figure 8 | AxMLP is necessary for initial cell proliferation during tail regeneration. **a-d**, Representative transverse sections of the morpholino-electroporated/protein-injected blastemas that were used for quantification of BrdU incorporation in Fig. 4d. Rhodamine was co-injected with the protein samples. **e**, Quantification of BrdU⁺ cells in blastema sections of morpholino-electroporated/protein-injected tails at 3 dpa ($n = 4$: biological replicates; centre values as median; points represent each sample). **f**, The length of the blastema during tail regeneration. The data at 6 dpa were plotted in Fig. 4c. By 14 days the difference in total regenerate length among the samples was not statistically significant. **g-j**, The same experimental scheme (shown in Fig. 4a) as was used for AxMLP morpholino 1 was implemented for a second specific morpholino (AxMLP-specific morpholino 2). **g**, Bright-field images of the morpholino-2-electroporated/

protein-injected tails at 6 dpa. Red bars indicate amputation planes. Dashed lines delineate the shape of the mesenchymal blastema. **h**, Blastema length at 6 dpa ($n = 4$: biological replicates; centre values as median; points represent each sample). **i**, The length of the blastema during tail regeneration. The data at 6 dpa were plotted in **h**. **j**, Transverse sections immunostained for BrdU from morpholino-electroporated/protein-injected tails at 3 dpa. AxMLP-specific morpholino 2 combined with flow-through (FT) injection shows reduction of BrdU incorporation, whereas AxMLP protein injection rescues the phenotype. The corresponding five-mismatch control morpholino does not affect BrdU incorporation. Yellow circles indicate spinal cord (top) and notochord/cartilage (bottom). NS, not significant; ** $P < 0.005$, *** $P < 0.0005$, **** $P < 0.00005$ with Student's *t*-test. Scale bars, 200 μ m (**a-d, j**); 500 μ m (**g**).



Extended Data Figure 9 | Anti-AxMLP antibody significantly blocks BrdU incorporation during tail regeneration. **a**, Schematic illustration of antibody injection into axolotl tail. **b**, Quantification of BrdU⁺ cells in blastema sections of antibody-injected tails at 3 dpa ($n = 4$: biological replicates; centre values as median; points represent each sample). NS, not significant; ** $P < 0.005$, *** $P < 0.0005$, **** $P < 0.00005$ with Student's *t*-test.



Extended Data Figure 10 | Exogenous AxMLP accelerates normal tail regeneration. **a**, Schematic illustration of the protein injection into axolotl tail and blastema. **b**, Bright-field images of the protein-injected tails at 4 dpa. **c**, Blastema length at 4 dpa ($n = 6$: PBS, FT; $n = 8$: AxMLP, biological replicates; centre values as median; points represent each sample). The

blastema from purified AxMLP injected tails significantly increased the regenerate length. Scale bar, 500 μm . Red bars indicate amputation planes; dashed lines delineate the shape of the mesenchymal blastema. NS, not significant; *** $P < 0.0005$ with Student's *t*-test.